Study on Function of Specific Region in p53-inducible Phosphatase PPM1D for Nucleolar Formation

（核小体形成における p53 誘導性ホスファターゼ PPM1D 特異的領域の機能に関する研究）

Graduate School of Chemical Sciences and Engineering,
Hokkaido University

Yuhei Kiyota

2017

Table of Contents

Abbreviations

Abbreviations:

ATM	ataxia telangiectasia mutated
CDC25	cell division cycle 25
CDK1	cyclin-dependent kinase 1
Chk1	checkpoint kinase 1
Chk2	checkpoint kinase 2
DAPI	4',6-diamidino-2-phenylindole, dihydrochloride
DFC	dense fibrillar component
DNA	deoxyribonucleic acid
EDTA	ethylenediaminetetraacetic acid
EGTA	ethylene glycol tetraacetic acid
FBS	fetal bovine serum
FC	fibrillar center
GC	granular component
HA	hemagglutinin
MAPK	mitogen-activated Protein Kinase
MCF7	michigan cancer foundation-7
NPM	nucleophosmin
NORs	nucleolus organizer regions
PAGE	polyacrylamide gel electrophoresis
PBS	phosphate buffered saline
PLK1	polo-like kinase 1
PPM1D	protein phosphatase 1D
PP1	protein phosphatase 1
PP2A	protein phosphatase 2A
rDNA	ribosomal DNA
RNA	ribonucleic acid
rRNA	ribosomal RNA
SDS	sodium dodecyl sulfate
TBS	tris-buffered saline
Tris	tris(hydroxymethyl)aminomethane

1. General introduction

1.1. Ser/Thr phosphatase PPM1D

PPM1D (protein phosphatase Mg^{2+}/Mn^{2+} dependent 1D, also known as PP2Cδ or Wip1) is a member of the PPM1 type Ser/Thr phosphatases. PPM1D was initially identified as a protein phosphatase induced by the tumor suppressor protein p53 after ionizing radiation (*1*). In the cellular response to ionizing radiation, PPM1D dephosphorylates and regulates p53 via a negative feedback loop (*2*). PPM1D also dephosphorylates ATM, p38 MAPK and Chk1/2, which are all involved in cellular responses to genotoxic stresses (*2-4*).

Studies in PPM1D knockout mice showed that PPM1D is involved in spermatogenesis and immune system. PPM1D-deficient mice show atrophy of testis and reduced male fertility (*5*). Deficiency of PPM1D impairs cellular function of T cells and B cells (*5*). In addition, PPM1D regulates differentiation of neutrophils and hematopoietic stem cell function (*6*).

Recent reports have indicated that PPM1D is also involved in metabolism. PPM1D controls the cellular response toward insulin by p53 activation (*7*). In macrophages of atherosclerosis, abnormal lipid metabolism is observed. PPM1D regulates formation of lipid droplets by dephosphorylation of ATM (*8*). Furthermore, inhibition of PPM1D promotes liver regeneration through activation of mTor, which is a key regulator of metabolism (*9*).

1.2. The *PPM1D* gene and its genetic mutation in human tumors

The *PPM1D* gene is located at 17q23.2 (**Figure 1-1**). Two types of *PPM1D*

mRNAs are produced from the primary transcript of the *PPM1D* gene. *PPM1D605* mRNA has contains six exons, exon 1, 2, 3, 4, 5 and 6, while *PPM1D430* is composed of exon 1, 2, 3, 4, 5, 5' and 6. *PPM1D430* is a splice variant, as reported by our group (*10*).

The chromosomal region *17q23* on which the gene *PPM1D* is located is frequently amplified in breast cancer (*11*). Overexpression of PPM1D and amplification of the *PPM1D* gene have been reported in various cancers, suggesting that PPM1D overexpression deeply involved in carcinogenesis (*12-23*) (**Table 1-1**). Overexpression of PPM1D is significantly associated with poorer clinical prognosis in gastric, lung and colorectal cancer (*19, 24-25*). These reports suggested that amplification of the *PPM1D* gene and overexpression of PPM1D protein are important factors to predict clinical prognosis and can help guide therapeutic options. Recent reports showed that protein-truncated variants in *PPM1D* are associated with predisposition to breast cancer and ovarian cancer (*26-27*). The truncation mutations of the PPM1D C-terminal domain stabilized PPM1D protein level, and stabilization of PPM1D increases its phosphatase activity (*28*). Importantly, phosphatase activity is an essential factor for its oncogenic activities (*29*). Together these studies indicate that PPM1D is an attractive therapeutic target and that its inhibitor may be a suitable candidate for an anticancer agent.

1.3. Structure of PPM1D

Protein phosphatases are classified into 6 groups with structural similarity (**Figure 1-2**) (*30-31*). PPM1D is a member of the PPM1 phosphatase family, which has 12 isoforms (**Figure 1-3**). The crystal structure of PPM1A was the first report in the PPM1 family (*32*). The active center of PPM1A consists of Asp, Glu and Arg with metal

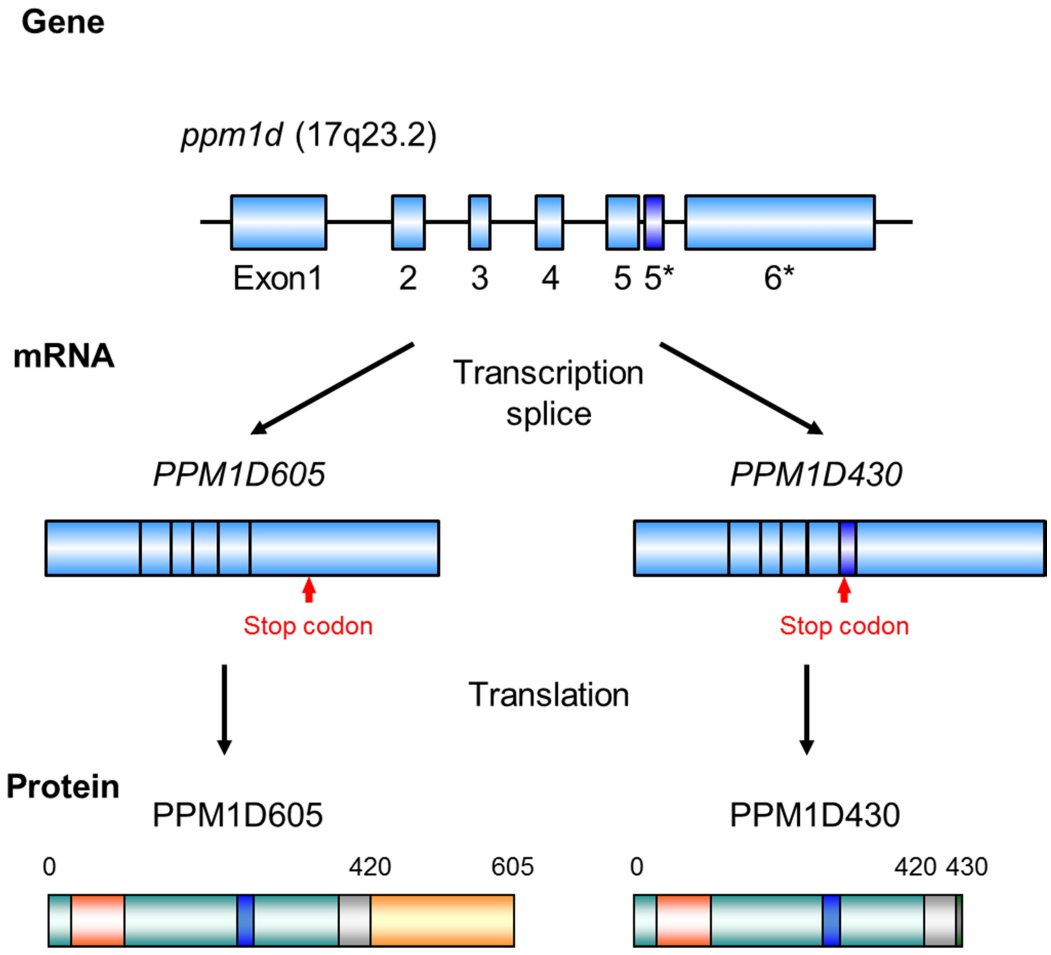

Figure 1-1 Schematic structures of PPM1D the gene, mRNA and Protein.

The *PPM1D* gene is located in 17q23.2. The *PPM1D* gene has 7 exons. Splice of PPM1D transcript produces two type of PPM1D mRNA, PPM1D605 and PPM1D430. Each splice variant of PPM1D has common catalytic domain and variant specific C-terminus regions. Figure 1-1 was reported Kamada *et al*. (*33*) and modified.

Table 1-1 Gene amplification, RNA overexpression and overexpression of *PPM1D* and PPM1D.

Tumors	Gene Amplification	RNA Overexpression	Protein Overexpression	Reference	
Breast cancer	37/326 (11%)			Bulavin *et al.*	[12]
	26/164 (16%)			Li *et al.*	[13]
	13/117 (11%)			Rauta *et al.*	[14]
		7/20 (35 %)		Yu *et al.*	[15]
	8/95 (8%)			Cerami *et al.*	[16]
	10/181 (6%)			Cerami *et al.*	[16]
Ovarian clear cell adenocarcinoma	8/20 (40%)			Hirasawa *et al.*	[17]
	9/89 (10%)			Gao J. *et al.*	[18]
Neuroblastoma	23/25 (92%)	9/32 (28%)		Saito *et al.*	[19]
	24/47 (51%)	148/168 (88%)		Mendrzyk *et al.*	[20]
Medulloblastoma	6/16 (37%)	3/11 (27%)		Ehrbrecht *et al.*	[21]
	7/11 (64%)	16/33 (48%)		Cerami *et al.*	[16]
Colorectal cancer		252/368 (68%)		Peng *et al.*	[22]
			102/120 (85%)	Li *et al.*	[13]
Pharyngeal cancer		58/85 (69%)		Cerami *et al.*	[16]
Renal cancer			53/78 (68%)	Cerami *et al.*	[16]
Lung cancer		52/75 (69%)		Cerami *et al.*	[16]
Liver cancer	23/25 (92%)	56/86 (65%)		Cerami et al.	[16]
Prostate cancer	0/3 (0%)	3/3 (100%)		Jiao *et al.*	[23]
Pancreatic cancer	8/13 (62%)	3/11 (27%)		Ehrbrecht *et al.*	[21]

In various tumors, Gene amplification, RNA overexpression and overexpression of *PPM1D* and PPM1D are reported. Table 1-1 was reported Kamada *et al*. (*33*) and modified.

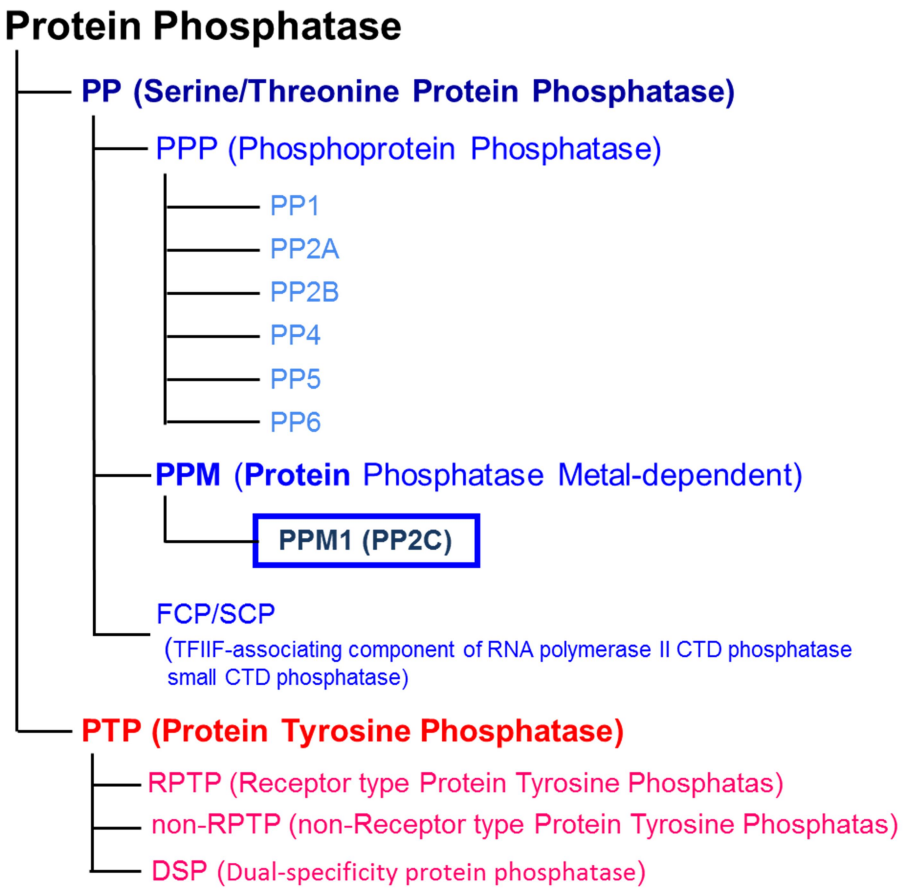

Figure 1-2 .Protein phosphatase groups.

Protein phosphatase is classified into two groups. One is Ser/Thr protein phosphatase and the other is Protein Tyr phosphatase. In Ser/Thr protein phosphatase, there are 7 families. PPM1D belongs to PPM1 family.

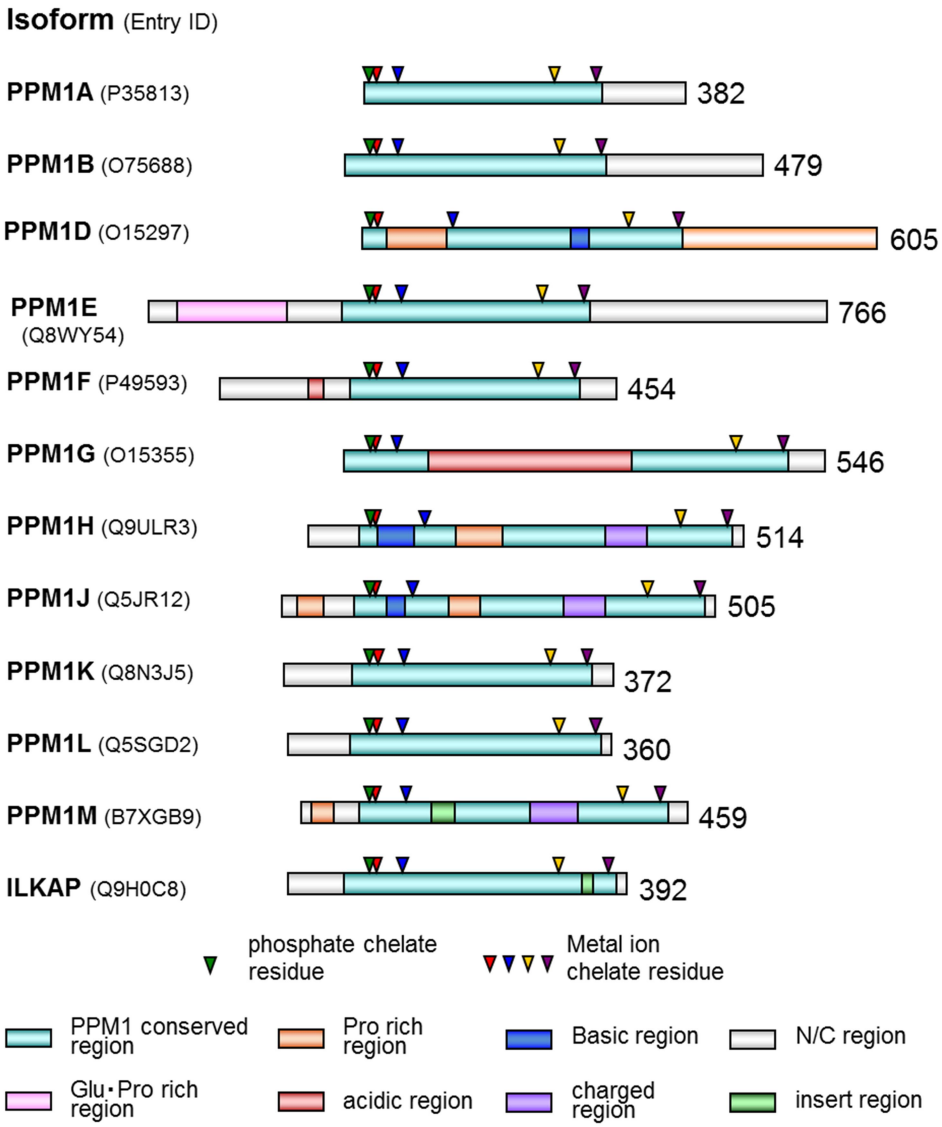

Figure 1-3 Structural scheme of PPM1 family isoforms.

Each PPM1 family has conserved catalytic domain. In catalytic domain, there are isoform specific insert region. N/C-terminus domain of each isoform is also isoform specific region. These regions should be involved in isoform specific regulation.

ions. Asp and Glu chelate Mg^{2+}/Mn^{2+} ion and Arg binds to phosphate (**Figure 1-4**). Structures of PPM1B and PPM1K have reported by Almo *et al*. (*34*). Comparison of the crystal structures of PPM1A (PDB ID: 1A6Q), PPM1B (PDB ID: 2P8E) and PPM1K (PDB ID: 2IQ1) revealed that the structures of the catalytic domain resemble each other. Alignment analysis revealed that amino acids in the active center are highly conserved among PPM1 family members. The sequences of the β-strand and α-helix, which are present in the catalytic domain, are also conserved. In addition, some isoforms have unique sequences between conserved regions and/or in the N/C-terminus. These specific regions may likely be involved in isoform-specific regulation (**Figure 1-3**).

PPM1D has a Pro-rich region and basic amino residue-rich region, named as the P-loop and B-loop, respectively, as unique regions in the catalytic domain. The P-loop is composed of 15 Pro residues within the 71 amino acid residues of the P-loop (**Figure 1-5**). The Pro-rich sequence is known as a protein-protein interaction sequence in various proteins (*35*), and PxP and PxxP motifs are typical motifs for protein-protein interactions. We previously reported that the B-loop is involved in PPM1D localization (*10*). Homology modeling of PPM1D revealed that the P-loop is located on the opposite side from the active center and the B-loop is close to the active center (**Figure 1-4**).

PPM1D605 and PPM1D430 have unique C-terminal regions (**Figure 1-6**). The functions of the C-terminal regions remain unknown. Recent studies suggested that the truncated mutation of PPM1D605 is a predisposition marker for tumors (*26, 36*). Ten residues in the C-terminal of PPM1D430 show similar sequences with p63 and p73, which are members of the p53 family. p73 interacts with c-Myc-binding protein MM1 and Trp-Asp repeat protein RACK1 via similar regions with PPM1D430 (*37-38*). Therefore, these regions may regulate PPM1D via protein-protein interactions.

1.4. PPM1D inhibitors

Many studies have been published on PPM1D inhibitors (**Table 1-2**). The inhibitors of PPM1D are classified into two types. One type includes the peptide derivative inhibitors, which are based on PPM1D substrates. Our group has reported a PPM1D inhibitor based on a substrate sequence of PPM1D (*39*). Two cyclic peptides are reported as PPM1D inhibitors with p38 MAPK sequences (*40-42*), and these inhibitors showed high specificity for PPM1D. However, the effects of the peptide analog compounds on PPM1D overexpressing tumors are unknown. The second type of PPM1D inhibitor includes the small molecule inhibitors. We reported a small molecule inhibitor SPI-001 that potently represses the proliferation of PPM1D overexpressing cells (*43*). CCT007093 and GSK2830371 are also small molecule inhibitors for PPM1D (*44-45*) and suppress proliferation of PPM1D overexpressing cancer cells. The inhibitors with high inhibitory activity, such as SPI-001, have a complex structure and are difficult to synthesize. Molecular weight is an important factor for drug design (*46*), as smaller compounds more easily penetrate the cell membrane. For development of an anti-cancer chemotherapy targeting PPM1D, simplification of compound structures with much higher inhibitory activity is required.

1.5. Nucleoli and cancer

The nucleolus is a structure within the nucleus that is involved in ribosomal biosynthesis, cell cycle regulation, DNA damage response and mRNA processing (*47-50*). Normal somatic cells have one to three nucleoli (*51-52*). The nucleolus consists of a fibrillary center (FC), dense fibrillar component (DFC) and granular component (GC) (**Figure 1-7**). These regions are divided by structural density, which can be

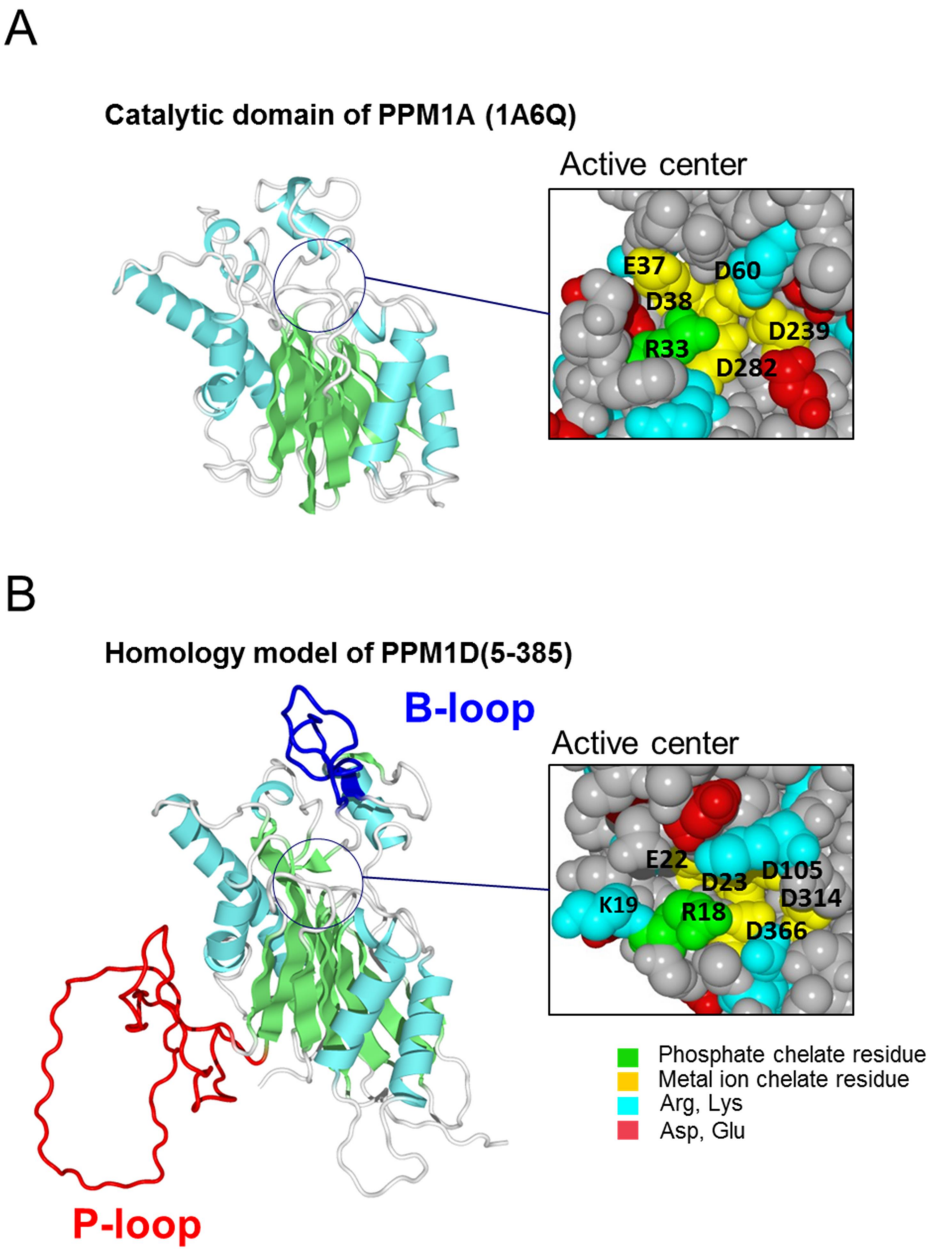

Figure 1-4 Structure of catalytic domain of PPM1A and PPM1D.

A) Crystal structure of PPM1A catalytic domain (PDB: 1A6Q). In active center, Arg33 residue is located as binding residue to phosphate group. Glu and Asp residues chelate metal ion. B) Homology model of PPM1D catalytic domain. structure of PPM1D estimated homology modeling with PPM1A, PPM1B and PPM1K crystal structure. P-loop is located in opposite from active center. B-loop is near from active center.

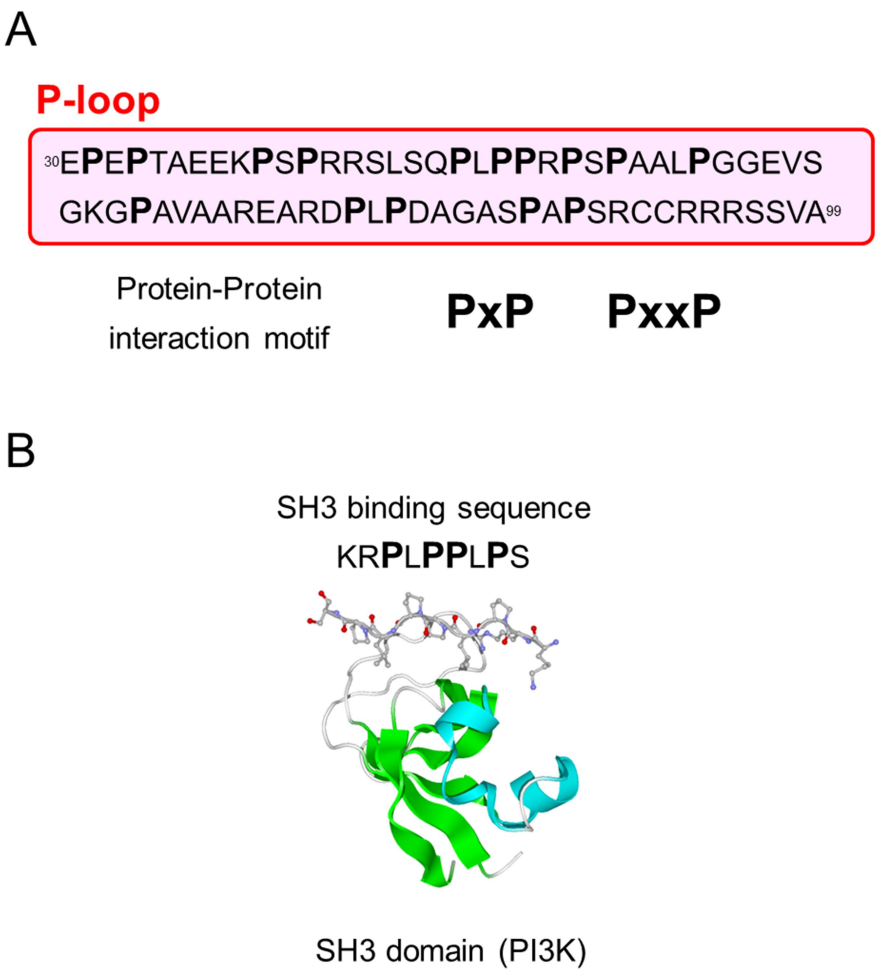

Figure 1-5 P-loop sequence and Pro-rich motif for protein-protein interaction.

A) P-loop has 13 Pro residues in 71 amino acids. PxP and PxxP motif are protein-protein interaction motif. B) A example of PxP and PxxP motif. SH3 domain binds with Pro-rich sequence which has PxP and PxxP motifs.

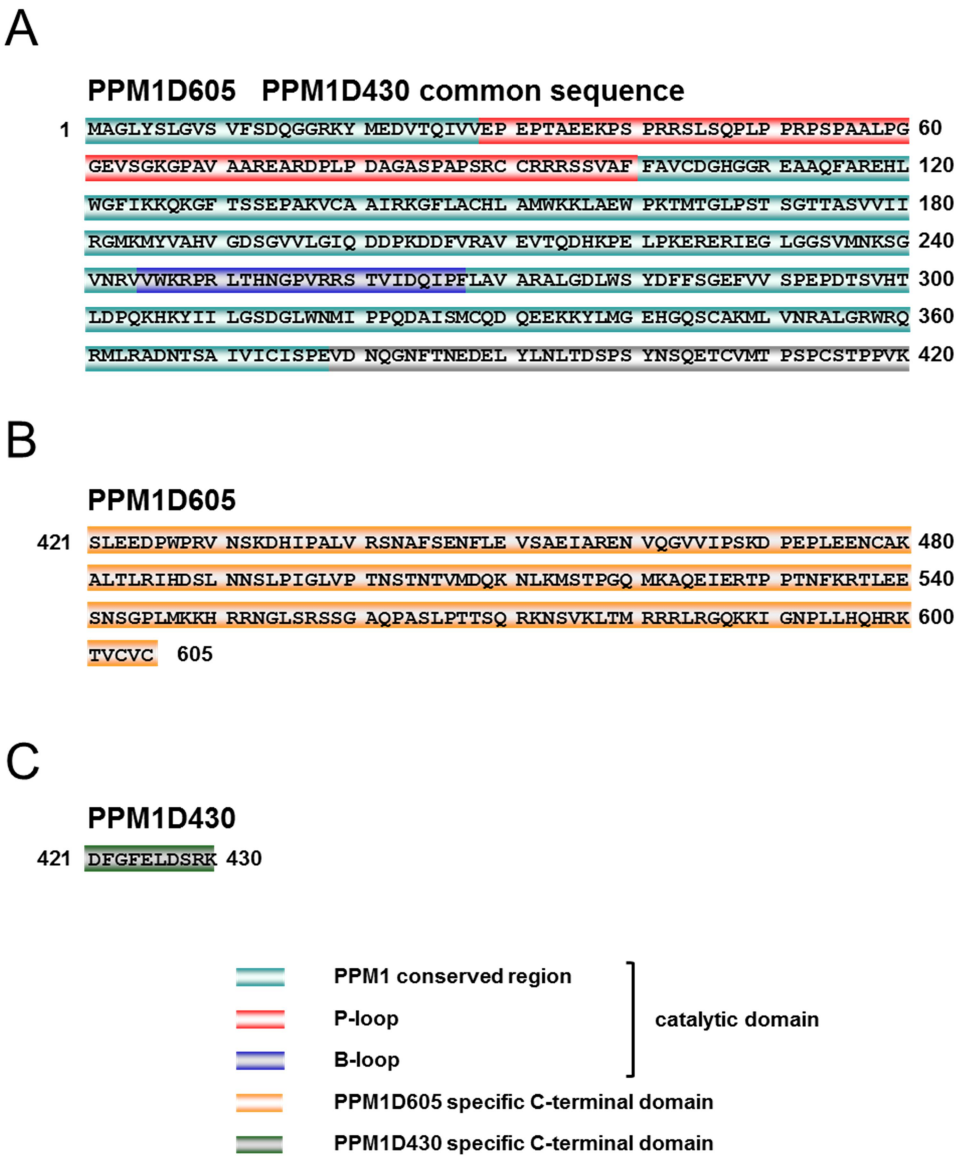

Figure 1-6 .Amino acid Sequence of PPM1D.

PPM1D605 and PPM1D430 have catalytic domain and variant specific regions. A)The catalytic domain is conserved among PPM1 family. On the other hand, PPM1D has PPM1D specific regions, Pro-rich loop (P-loop) and basic amino rich loop (B-loop). B) PPM1D605 specific C-terminal domains C) PPM1D430 specific sequence C-terminal domains

Table 1-2 Summary of PPM1D inhibitors which are reported.

Inhibitor	Structure	IC_{50}	References	
SPI-001	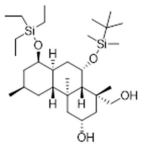	0.48 (μM)	Yagi *et al*.	[43]
AP4-3E-A	**Ac-VEPPL(AP4)QEEEEDLW-NH_2**	7.8 (μM)	Chuman *et al*.	[39]
Not determined	**c(MS(P)IY(P)VA)**	3.7 (μM)	Yamaguchi *et al*.	[40]
Not determined	**c(FS(P)IY(P)DD)**	0.1 (μM)	Hayashi *et al*.	[41]
GSK2830371	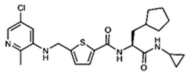	6 (nM)	Gilmartin *et al*.	[45]
CCT007093	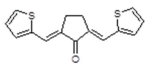	8.4 (μM)	Rayter *et al*.	[44]
CCT071835	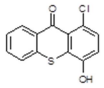	1.5 (μM)	Rayter *et al*.	[44]
CCT021600	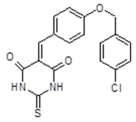	4.7 (μM)	Rayter *et al*.	[44]
CCT010971	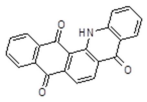	6.1 (μM)	Rayter *et al*.	[44]
Not determined	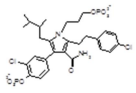	9.8 (μM)	Bang *et al*.	[42]

Values of IC_{50} are toward PPM1D enzyme.

observed with electron microscopy (*53*). Nucleolus organizer regions (NORs) are located in the nucleolar center and are chromosomal regions coding rRNA genes.

In many types of tumors, increases of nucleolar number have been reported (*54-55*). The number of nucleoli is an important criterion in the cytodiagnosis of tumors (*56*). Abnormal nucleolar morphologies, such as increases of number and size, are observed in malignant tumors. Additionally, variability of nucleolar morphologies in tumor tissue is also a character of malignancy. Therefore, abnormal morphology of nucleoli should be associated with tumorigenesis.

1.6. Nucleolar protein nucleophosmin

Nucleophosmin (NPM, also known as B23 and numatrin) is a nucleolar protein of 294 amino acids (*57*) (**Figure 1-8**). NPM is composed of an oligomeric domain, acidic domain and DNA/RNA binding domain. NPM is expressed ubiquitously in human tissues and knockout mice of NPM are lethal (*58*). Hence, NPM likely has essential roles for cell survival. NPM regulates ribosomal biosynthesis, cell cycle regulation and centrosome duplication (*59-60*). Overexpression of NPM is frequently observed in solid tumors (*61*). In hematopoietic stem cell tumors, chimeric NPM proteins that show translocation of *NPM* are reported. Therefore, abnormal regulation of NPM should be associated with tumorigenesis.

Proteomics analysis showed that NPM is highly phosphorylated (*52, 62-64*). Ser4 and Thr199 of NPM are phosphorylated by PLK-1 and CDK-1 kinase, respectively (*59, 65*). Our group reported that phosphorylation of NPM on Ser4 and Thr199 increases the nucleolar number (*66*). Notably, overexpression of PPM1D activates the CDC25C-CDK1-PLK1 pathway (**Figure 1-9**). PPM1D activates CDC25C via a

p53-independent and/or p53-dependent manner. CDC25C dephosphorylates and activates CDK1, and CDK1 phosphorylates Thr199 in NPM and then PLK1 subsequently phosphorylates Ser4 of NPM. However, the molecular mechanisms underlying the phosphorylation of Ser4 and Thr199 and the increase of nucleolar number are still unknown.

Previous studies reported that NPM forms decamers (*67-68*) (**Figure 1-10**). The structural analysis results led to a hypothesis that the phosphorylation state of NPM may affect its oligomeric formation (*67*). Formation of decamers is essential for the interaction between NPM and histone (*68-69*). However, the relationship of oligomeric formation and function of NPM has not been reported.

1.7. Nucleolus formation and the cell cycle

Nucleoli show dynamic changes in number and shape depending on the cell cycle progression (*70*) (**Figure 1-11**). In the mitotic phase, the nucleolus is disassembled. Nucleolar proteins, including NPM, translocate to the cytoplasm and/or chromatin. Then, the nucleolus reforms on NORs in early G1 phase. In early G1 phase, proteins that compose the GC and DFG start to associate into the pre-nucleolus body (PNB) apart from NORs (*71*). Throughout progression of G1 phase, NORs fuse and begin to increase in size, while PNBs increase in size and then disappear. PNBs do not fuse with NORs or each other (*52*). PNB-associated factors dissociate from PNBs and are recruited to NORs.

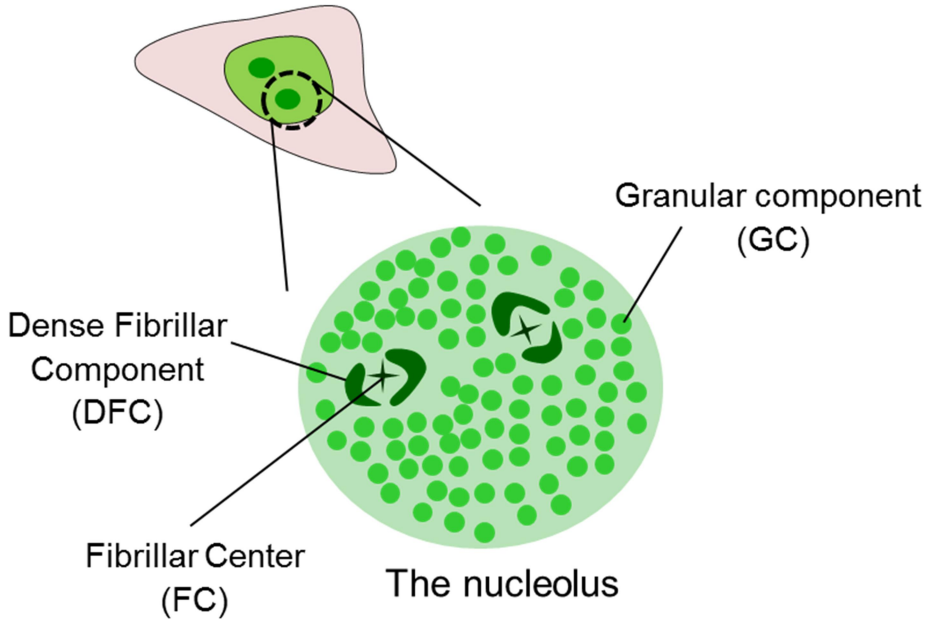

Figure 1-7 Model of the nucleolus structure.

The nucleolus is composed with fibrillary center (FC), dense fibrillar component (DFC) and Granular component (GC). DFC has nucleolus organizer regions (NORs) which is chromosomal region coding rRNA.

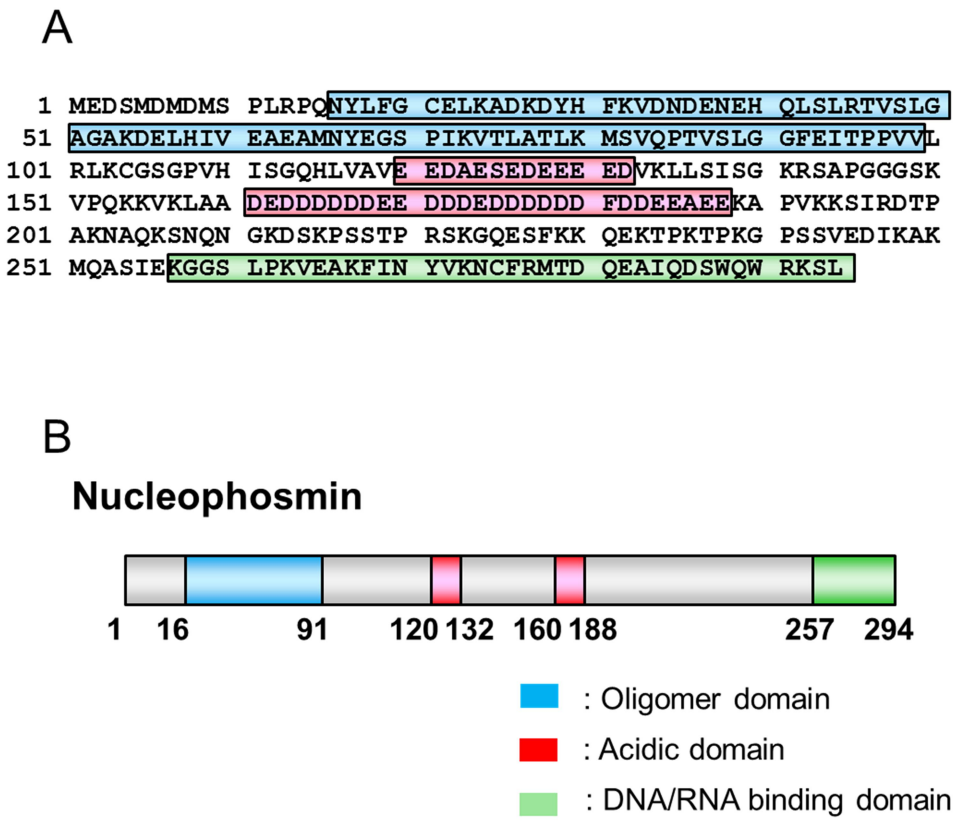

Figure 1-8 Protein sequence and schematic structure of NPM.

A) NPM is comsist of 294 amino acids. B) NPM has oligomer domain, acidic domain and DNA/RNA binding domain.

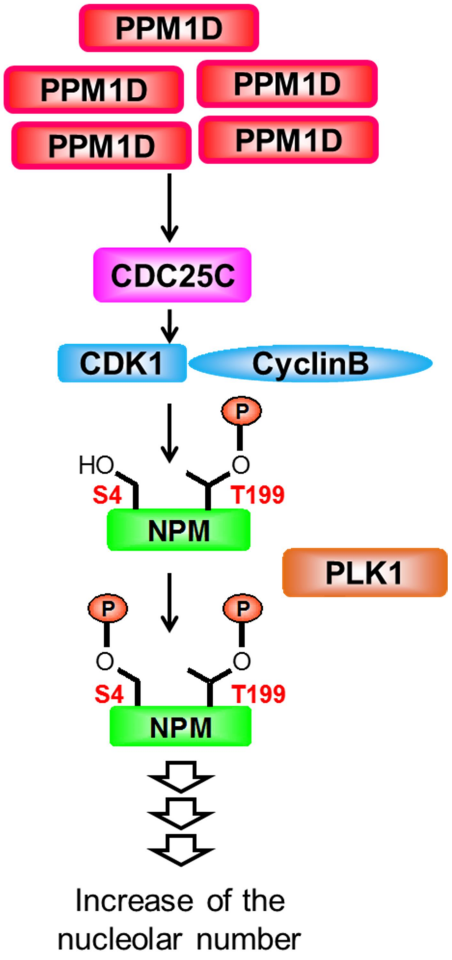

Figure 1-9 Increase of the nucleolar number by overexpressed PPM1D.

NPM was phosphorylated at Ser4 and Thr 199 sequentially. PPM1D overexpression activates CDC25C phosphatase. CDK1-cyclineB activated by CDC25C phosphorylates NPM at Thr199. PLK1 recognizes phosphorylated Thr199 of NPM and phosphorylatesSer4 of NPM. Phosphorylated NPM increases the nucleolar number. However the molecule mechanism is still known. This figure was reported Kozakai *et al*. (*66*) and modified.

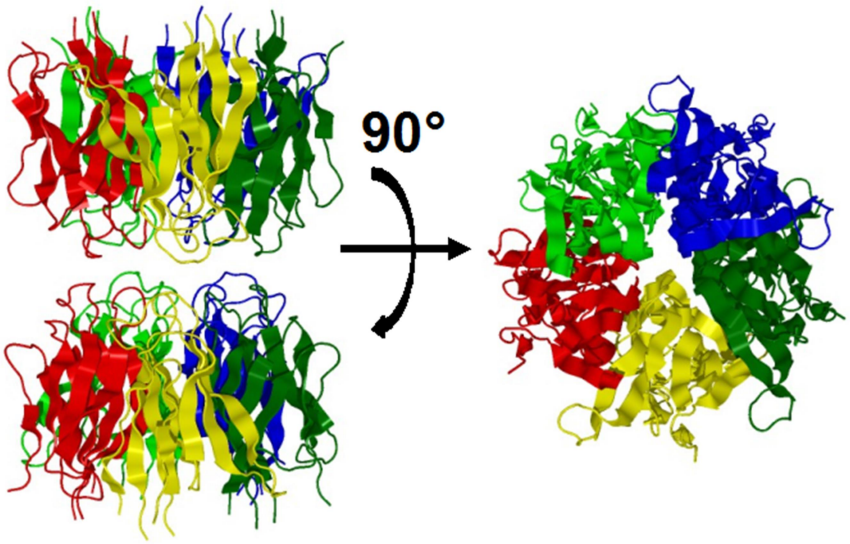

Figure 1-10 Crystal structure of NPM oligomerization domain (PDB: 2P1B).
Oligomerization domain of NPM (15-118) forms decamer. Decamer is a dimer of pentamers.

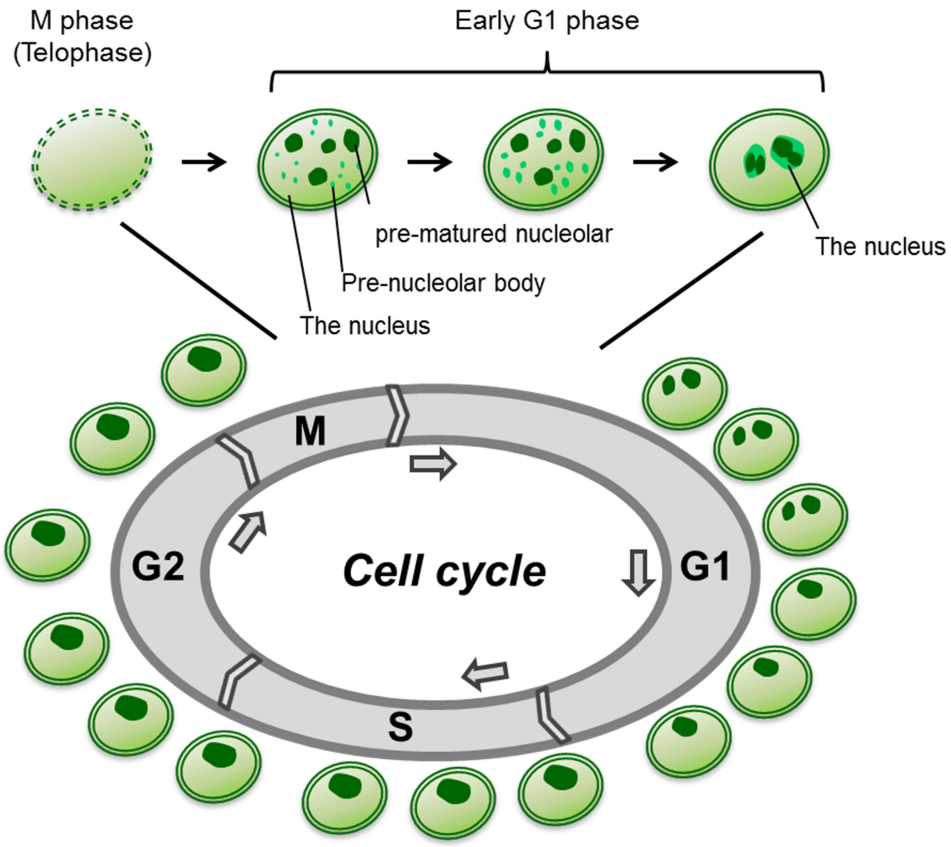

Figure 1-10 The nucleolar assembly depending on cell cycle.

The nucleolus rebuilds in early G1 phase. In the end of telophase, NORs recruit nucleolar factors. Pre-nucleolar body (PNB) also forms in G1 phase. GC and DFC component factors, such as NPM, associate in PNB. As progress of G1 phase, PNB grow up and disassembly. At the same time, prenucleolar bind each other with GC and DFC component factors which disassociated with PNB.

1.8. Aim of this study

Many reports suggested that PPM1D is proto-oncogene and is associated with tumorigenesis. Inhibition of PPM1D phosphatase activity is a promising target of anti-cancer chemotherapy. Cytodiagnosis of tumors shows an increase of the nucleolar number. Our previous study demonstrated that overexpression of PPM1D increases the nucleolus number via phosphorylation of NPM. The CDC25-CDK1-PLK1 pathway activated by PPM1D phosphorylates Ser4 and Thr199 of NPM. However, the molecular mechanisms of nucleolar formation as regulated by PPM1D are still unknown. Moreover, the regulation mechanism of PPM1D itself is also unknown. In this study, I developed a novel PPM1D inhibitor and revealed the mechanism of nucleolar formation regulated by a specific region in PPM1D, the P-loop.

1.9. References

1. M. Fiscella, H. Zhang, S. Fan, K. Sakaguchi, S. Shen, W. E. Mercer, G. F. Vande Woude, P. M. O'Connor, E. Appella (1997) Wip1, a novel human protein phosphatase that is induced in response to ionizing radiation in a p53-dependent manner Proc Natl Acad Sci U S A, 94, 6048-6053.
2. M. Takekawa, M. Adachi, A. Nakahata, I. Nakayama, F. Itoh, H. Tsukuda, Y. Taya, K. Imai (2000) p53-inducible wip1 phosphatase mediates a negative feedback regulation of p38 MAPK-p53 signaling in response to UV radiation EMBO J, 19, 6517-6526.
3. X. Lu, T. A. Nguyen, L. A. Donehower (2005) Reversal of the ATM/ATR-mediated DNA damage response by the oncogenic phosphatase PPM1D Cell Cycle, 4, 1060-1064.
4. X. Lu, B. Nannenga, L. A. Donehower (2005) PPM1D dephosphorylates Chk1 and p53 and abrogates cell cycle checkpoints Genes Dev, 19, 1162-1174.
5. J. Choi, B. Nannenga, O. N. Demidov, D. V. Bulavin, A. Cooney, C. Brayton, Y. Zhang, I. N. Mbawuike, A. Bradley, E. Appella, L. A. Donehower (2002) Mice Deficient for the Wild-Type p53-Induced Phosphatase Gene (Wip1) Exhibit Defects in Reproductive Organs, Immune Function, and Cell Cycle Control Molecular and Cellular Biology, 22, 1094-1105.
6. Z. Chen, W. Yi, Y. Morita, H. Wang, Y. Cong, J. P. Liu, Z. Xiao, K. L. Rudolph, T. Cheng, Z. Ju (2015) Wip1 deficiency impairs haematopoietic stem cell function via p53 and mTORC1 pathways Nat Commun, 6, 6808.
7. H. L. Armata, S. Chamberland, L. Watts, H. J. Ko, Y. Lee, D. Y. Jung, J. K. Kim, H. K. Sluss (2015) Deficiency of the tumor promoter gene wip1 induces insulin resistance Mol Endocrinol, 29, 28-39.
8. X. Le Guezennec, A. Brichkina, Y. F. Huang, E. Kostromina, W. Han, D. V. Bulavin (2012) Wip1-dependent regulation of autophagy, obesity, and atherosclerosis Cell Metab, 16, 68-80.
9. L. Zhang, L. Liu, Z. He, G. Li, J. Liu, Z. Song, H. Jin, K. L. Rudolph, H. Yang, Y. Mao, L. Zhang, H. Zhang, Z. Xiao, Z. Ju (2015) Inhibition of wild-type p53-induced phosphatase 1 promotes liver regeneration in mice by direct activation of mammalian target of rapamycin Hepatology, 61, 2030-2041.
10. Y. Chuman, W. Kurihashi, Y. Mizukami, T. Nashimoto, H. Yagi, K. Sakaguchi (2009) PPM1D430, a novel alternative splicing variant of the human PPM1D, can dephosphorylate p53 and exhibits specific tissue expression J Biochem, 145, 1-12.
11. Z. Varga, C. B. Moelans, U. Zuerrer-Hardi, C. Ramach, S. Behnke, G. Kristiansen, H. Moch (2012) Topoisomerase 2A gene amplification in breast cancer. Critical evaluation of different FISH probes Breast Cancer Res Treat, 133, 929-935.
12. D. V. Bulavin, O. N. Demidov, S. Saito, P. Kauraniemi, C. Phillips, S. A. Amundson, C. Ambrosino, G. Sauter, A. R. Nebreda, C. W. Anderson, A. Kallioniemi, A. J. Fornace, Jr., E.

Appella (2002) Amplification of PPM1D in human tumors abrogates p53 tumor-suppressor activity Nat Genet, 31, 210-215.

13. Z. T. Li, L. Zhang, X. Z. Gao, X. H. Jiang, L. Q. Sun (2013) Expression and significance of the Wip1 proto-oncogene in colorectal cancer Asian Pac J Cancer Prev, 14, 1975-1979.
14. J. Rauta, E. L. Alarmo, P. Kauraniemi, R. Karhu, T. Kuukasjarvi, A. Kallioniemi (2006) The serine-threonine protein phosphatase PPM1D is frequently activated through amplification in aggressive primary breast tumours Breast Cancer Res Treat, 95, 257-263.
15. E. Yu, Y. S. Ahn, S. J. Jang, M. J. Kim, H. S. Yoon, G. Gong, J. Choi (2007) Overexpression of the wip1 gene abrogates the p38 MAPK/p53/Wip1 pathway and silences p16 expression in human breast cancers Breast Cancer Res Treat, 101, 269-278.
16. E. Cerami, J. Gao, U. Dogrusoz, B. E. Gross, S. O. Sumer, B. A. Aksoy, A. Jacobsen, C. J. Byrne, M. L. Heuer, E. Larsson, Y. Antipin, B. Reva, A. P. Goldberg, C. Sander, N. Schultz (2012) The cBio cancer genomics portal: an open platform for exploring multidimensional cancer genomics data Cancer Discov, 2, 401-404.
17. A. Hirasawa, F. Saito-Ohara, J. Inoue, D. Aoki, N. Susumu, T. Yokoyama, S. Nozawa, J. Inazawa, I. Imoto (2003) Association of 17q21-q24 gain in ovarian clear cell adenocarcinomas with poor prognosis and identification of PPM1D and APPBP2 as likely amplification targets Clin Cancer Res, 9, 1995-2004.
18. J. Gao, B. A. Aksoy, U. Dogrusoz, G. Dresdner, B. Gross, S. O. Sumer, Y. Sun, A. Jacobsen, R. Sinha, E. Larsson, E. Cerami, C. Sander, N. Schultz (2013) Integrative analysis of complex cancer genomics and clinical profiles using the cBioPortal Sci Signal, 6, pl1.
19. F. Saito-Ohara, I. Imoto, J. Inoue, H. Hosoi, A. Nakagawara, T. Sugimoto, J. Inazawa (2003) PPM1D is a potential target for 17q gain in neuroblastoma Cancer Res, 63, 1876-1883.
20. F. Mendrzyk, B. Radlwimmer, S. Joos, F. Kokocinski, A. Benner, D. E. Stange, K. Neben, H. Fiegler, N. P. Carter, G. Reifenberger, A. Korshunov, P. Lichter (2005) Genomic and protein expression profiling identifies CDK6 as novel independent prognostic marker in medulloblastoma J Clin Oncol, 23, 8853-8862.
21. A. Ehrbrecht, U. Muller, M. Wolter, A. Hoischen, A. Koch, B. Radlwimmer, B. Actor, A. Mincheva, T. Pietsch, P. Lichter, G. Reifenberger, R. G. Weber (2006) Comprehensive genomic analysis of desmoplastic medulloblastomas: identification of novel amplified genes and separate evaluation of the different histological components J Pathol, 208, 554-563.
22. T. S. Peng, Y. H. He, T. Nie, X. D. Hu, H. Y. Lu, J. Yi, Y. F. Shuai, M. Luo (2014) PPM1D is a prognostic marker and therapeutic target in colorectal cancer Exp Ther Med, 8, 430-434.
23. L. Jiao, D. Shen, G. Liu, J. Jia, J. Geng, H. Wang, Y. Sun (2014) PPM1D as a novel biomarker for prostate cancer after radical prostatectomy Anticancer Res, 34, 2919-2925.
24. G. B. Li, X. L. Zhang, L. Yuan, Q. Q. Jiao, D. J. Liu, J. Liu (2013) Protein phosphatase

magnesium-dependent 1delta (PPM1D) mRNA expression is a prognosis marker for hepatocellular carcinoma PLoS One, 8, e60775.

25. D. S. Tan, M. B. Lambros, S. Rayter, R. Natrajan, R. Vatcheva, Q. Gao, C. Marchio, F. C. Geyer, K. Savage, S. Parry, K. Fenwick, N. Tamber, A. Mackay, T. Dexter, C. Jameson, W. G. McCluggage, A. Williams, A. Graham, D. Faratian, M. El-Bahrawy, A. J. Paige, H. Gabra, M. E. Gore, M. Zvelebil, C. J. Lord, S. B. Kaye, A. Ashworth, J. S. Reis-Filho (2009) PPM1D is a potential therapeutic target in ovarian clear cell carcinomas Clin Cancer Res, 15, 2269-2280.
26. E. Ruark, K. Snape, P. Humburg, C. Loveday, I. Bajrami, R. Brough, D. N. Rodrigues, A. Renwick, S. Seal, E. Ramsay, V. Duarte Sdel, M. A. Rivas, M. Warren-Perry, A. Zachariou, A. Campion-Flora, S. Hanks, A. Murray, N. Ansari Pour, J. Douglas, L. Gregory, A. Rimmer, N. M. Walker, T. P. Yang, J. W. Adlard, J. Barwell, J. Berg, A. F. Brady, C. Brewer, G. Brice, C. Chapman, J. Cook, R. Davidson, A. Donaldson, F. Douglas, D. Eccles, D. G. Evans, L. Greenhalgh, A. Henderson, L. Izatt, A. Kumar, F. Lalloo, Z. Miedzybrodzka, P. J. Morrison, J. Paterson, M. Porteous, M. T. Rogers, S. Shanley, L. Walker, M. Gore, R. Houlston, M. A. Brown, M. J. Caufield, P. Deloukas, M. I. McCarthy, J. A. Todd, Breast, C. Ovarian Cancer Susceptibility, C. Wellcome Trust Case Control, C. Turnbull, J. S. Reis-Filho, A. Ashworth, A. C. Antoniou, C. J. Lord, P. Donnelly, N. Rahman (2013) Mosaic PPM1D mutations are associated with predisposition to breast and ovarian cancer Nature, 493, 406-410.
27. L. Zhang, L. H. Chen, H. Wan, R. Yang, Z. Wang, J. Feng, S. Yang, S. Jones, S. Wang, W. Zhou, H. Zhu, P. J. Killela, J. Zhang, Z. Wu, G. Li, S. Hao, Y. Wang, J. B. Webb, H. S. Friedman, A. H. Friedman, R. E. McLendon, Y. He, Z. J. Reitman, D. D. Bigner, H. Yan (2014) Exome sequencing identifies somatic gain-of-function PPM1D mutations in brainstem gliomas Nat Genet, 46, 726-730.
28. P. Kleiblova, I. A. Shaltiel, J. Benada, J. Sevcik, S. Pechackova, P. Pohlreich, E. E. Voest, P. Dundr, J. Bartek, Z. Kleibl, R. H. Medema, L. Macurek (2013) Gain-of-function mutations of PPM1D/Wip1 impair the p53-dependent G1 checkpoint J Cell Biol, 201, 511-521.
29. X. Zhang, G. Wan, S. Mlotshwa, V. Vance, F. G. Berger, H. Chen, X. Lu (2010) Oncogenic Wip1 phosphatase is inhibited by miR-16 in the DNA damage signaling pathway Cancer Res, 70, 7176-7186.
30. Y. Shi (2009) Serine/threonine phosphatases: mechanism through structure Cell, 139, 468-484.
31. S. J. Kim, S. E. Ryu (2012) Structure and catalytic mechanism of human protein tyrosine phosphatome BMB Rep, 45, 693-699.
32. A. K. Das, N. R. Helps, P. T. Cohen, D. Barford (1996) Crystal structure of the protein serine/threonine phosphatase 2C at 2.0 A resolution EMBO J, 15, 6798-6809.
33. R. Kamada, Y. Chuman, Y. Kozakai, K. Sakaguchi (2015) [Function of Proto-oncogene Product PPM1D and Development of PPM1D Inhibitors for Cancer Chemotherapy] Seikagaku, 87,

531-538.

34. S. C. Almo, J. B. Bonanno, J. M. Sauder, S. Emtage, T. P. Dilorenzo, V. Malashkevich, S. R. Wasserman, S. Swaminathan, S. Eswaramoorthy, R. Agarwal, D. Kumaran, M. Madegowda, S. Ragumani, Y. Patskovsky, J. Alvarado, U. A. Ramagopal, J. Faber-Barata, M. R. Chance, A. Sali, A. Fiser, Z. Y. Zhang, D. S. Lawrence, S. K. Burley (2007) Structural genomics of protein phosphatases J Struct Funct Genomics, 8, 121-140.
35. M. P. Williamson (1994) The structure and function of proline-rich regions in proteins Biochem J, 297 (Pt 2), 249-260.
36. Y. Kozakai, R. Kamada, Y. Kiyota, F. Yoshimura, K. Tanino, K. Sakaguchi (2014) Inhibition of C-terminal truncated PPM1D enhances the effect of doxorubicin on cell viability in human colorectal carcinoma cell line Bioorg Med Chem Lett, 24, 5593-5596.
37. K. Watanabe, T. Ozaki, T. Nakagawa, K. Miyazaki, M. Takahashi, M. Hosoda, S. Hayashi, S. Todo, A. Nakagawara (2002) Physical interaction of p73 with c-Myc and MM1, a c-Myc-binding protein, and modulation of the p73 function J Biol Chem, 277, 15113-15123.
38. T. Ozaki, K. Watanabe, T. Nakagawa, K. Miyazaki, M. Takahashi, A. Nakagawara (2003) Function of p73, not of p53, is inhibited by the physical interaction with RACK1 and its inhibitory effect is counteracted by pRB Oncogene, 22, 3231-3242.
39. Y. Chuman, H. Yagi, T. Fukuda, T. Nomura, M. Matsukizono, Y. Shimohigashi, K. Sakaguchi (2008) Characterization of the active site and a unique uncompetitive inhibitor of the PPM1-type protein phosphatase PPM1D Protein Pept Lett, 15, 938-948.
40. H. Yamaguchi, S. R. Durell, H. Feng, Y. Bai, C. W. Anderson, E. Appella (2006) Development of a substrate-based cyclic phosphopeptide inhibitor of protein phosphatase 2Cdelta, Wip1 Biochemistry, 45, 13193-13202.
41. R. Hayashi, K. Tanoue, S. R. Durell, D. K. Chatterjee, L. M. Jenkins, D. H. Appella, E. Appella (2011) Optimization of a cyclic peptide inhibitor of Ser/Thr phosphatase PPM1D (Wip1) Biochemistry, 50, 4537-4549.
42. J. Bang, H. Yamaguchi, S. R. Durell, E. Appella, D. H. Appella (2008) A small molecular scaffold for selective inhibition of Wip1 phosphatase ChemMedChem, 3, 230-232.
43. H. Yagi, Y. Chuman, Y. Kozakai, T. Imagawa, Y. Takahashi, F. Yoshimura, K. Tanino, K. Sakaguchi (2012) A small molecule inhibitor of p53-inducible protein phosphatase PPM1D Bioorg Med Chem Lett, 22, 729-732.
44. S. Rayter, R. Elliott, J. Travers, M. G. Rowlands, T. B. Richardson, K. Boxall, K. Jones, S. Linardopoulos, P. Workman, W. Aherne, C. J. Lord, A. Ashworth (2008) A chemical inhibitor of PPM1D that selectively kills cells overexpressing PPM1D Oncogene, 27, 1036-1044.
45. A. G. Gilmartin, T. H. Faitg, M. Richter, A. Groy, M. A. Seefeld, M. G. Darcy, X. Peng, K. Federowicz, J. Yang, S. Y. Zhang, E. Minthorn, J. P. Jaworski, M. Schaber, S. Martens, D. E.

McNulty, R. H. Sinnamon, H. Zhang, R. B. Kirkpatrick, N. Nevins, G. Cui, B. Pietrak, E. Diaz, A. Jones, M. Brandt, B. Schwartz, D. A. Heerding, R. Kumar (2014) Allosteric Wip1 phosphatase inhibition through flap-subdomain interaction Nat Chem Biol, 10, 181-187.

46. C. A. Lipinski, F. Lombardo, B. W. Dominy, P. J. Feeney (2012) Experimental and computational approaches to estimate solubility and permeability in drug discovery and development settings Advanced Drug Delivery Reviews, 64, 4-17.
47. A. Fatica, D. Tollervey (2002) Making ribosomes Curr Opin Cell Biol, 14, 313-318.
48. R. Visintin, A. Amon (2000) The nucleolus: the magician's hat for cell cycle tricks Curr Opin Cell Biol, 12, 752.
49. D. Bertwistle, M. Sugimoto, C. J. Sherr (2004) Physical and functional interactions of the Arf tumor suppressor protein with nucleophosmin/B23 Mol Cell Biol, 24, 985-996.
50. J. S. Andersen, Y. W. Lam, A. K. Leung, S. E. Ong, C. E. Lyon, A. I. Lamond, M. Mann (2005) Nucleolar proteome dynamics Nature, 433, 77-83.
51. J. R. Shea, Jr., C. P. Leblond (1966) Number of nucleoli in various cell types of the mouse J Morphol, 119, 425-433.
52. D. Hernandez-Verdun (2011) Assembly and disassembly of the nucleolus during the cell cycle Nucleus, 2, 189-194.
53. D. Hernandez-Verdun (2006) The nucleolus: a model for the organization of nuclear functions Histochem Cell Biol, 126, 135-148.
54. D. Ruggero, P. P. Pandolfi (2003) Does the ribosome translate cancer? Nat Rev Cancer, 3, 179-192.
55. M. Derenzini, L. Montanaro, D. Trere (2009) What the nucleolus says to a tumour pathologist Histopathology, 54, 753-762.
56. D. Ruggero (2012) Revisiting the nucleolus: from marker to dynamic integrator of cancer signaling Sci Signal, 5, pe38.
57. D. M. Mitrea, C. R. Grace, M. Buljan, M. K. Yun, N. J. Pytel, J. Satumba, A. Nourse, C. G. Park, M. Madan Babu, S. W. White, R. W. Kriwacki (2014) Structural polymorphism in the N-terminal oligomerization domain of NPM1 Proc Natl Acad Sci U S A, 111, 4466-4471.
58. S. Grisendi, R. Bernardi, M. Rossi, K. Cheng, L. Khandker, K. Manova, P. P. Pandolfi (2005) Role of nucleophosmin in embryonic development and tumorigenesis Nature, 437, 147-153.
59. H. Zhang, X. Shi, H. Paddon, M. Hampong, W. Dai, S. Pelech (2004) B23/nucleophosmin serine 4 phosphorylation mediates mitotic functions of polo-like kinase 1 J Biol Chem, 279, 35726-35734.
60. W. Du, Y. Zhou, S. Pike, Q. Pang (2010) NPM phosphorylation stimulates Cdk1, overrides G2/M checkpoint and increases leukemic blasts in mice Carcinogenesis, 31, 302-310.
61. S. Grisendi, C. Mecucci, B. Falini, P. P. Pandolfi (2006) Nucleophosmin and cancer Nat Rev

Cancer, 6, 493-505.

62. K. H. Tsui, A. J. Cheng, P. Chang, T. L. Pan, B. Y. Yung (2004) Association of nucleophosmin/B23 mRNA expression with clinical outcome in patients with bladder carcinoma Urology, 64, 839-844.
63. M. Hisaoka, S. Ueshima, K. Murano, K. Nagata, M. Okuwaki (2010) Regulation of nucleolar chromatin by B23/nucleophosmin jointly depends upon its RNA binding activity and transcription factor UBF Mol Cell Biol, 30, 4952-4964.
64. R. L. Redner, E. A. Rush, S. Faas, W. A. Rudert, S. J. Corey (1996) The t(5;17) variant of acute promyelocytic leukemia expresses a nucleophosmin-retinoic acid receptor fusion Blood, 87, 882-886.
65. M. Peter, J. Nakagawa, M. Doree, J. C. Labbe, E. A. Nigg (1990) Identification of major nucleolar proteins as candidate mitotic substrates of cdc2 kinase Cell, 60, 791-801.
66. Y. Kozakai, R. Kamada, J. Furuta, Y. Kiyota, Y. Chuman, K. Sakaguchi (2016) PPM1D controls nucleolar formation by up-regulating phosphorylation of nucleophosmin Sci Rep, 6, 33272.
67. H. H. Lee, H. S. Kim, J. Y. Kang, B. I. Lee, J. Y. Ha, H. J. Yoon, S. O. Lim, G. Jung, S. W. Suh (2007) Crystal structure of human nucleophosmin-core reveals plasticity of the pentamer-pentamer interface Proteins, 69, 672-678.
68. M. Okuwaki, A. Sumi, M. Hisaoka, A. Saotome-Nakamura, S. Akashi, Y. Nishimura, K. Nagata (2012) Function of homo- and hetero-oligomers of human nucleoplasmin/nucleophosmin family proteins NPM1, NPM2 and NPM3 during sperm chromatin remodeling Nucleic Acids Res, 40, 4861-4878.
69. O. Platonova, I. V. Akey, J. F. Head, C. W. Akey (2011) Crystal structure and function of human nucleoplasmin (npm2): a histone chaperone in oocytes and embryos Biochemistry, 50, 8078-8089.
70. F. M. Boisvert, S. van Koningsbruggen, J. Navascues, A. I. Lamond (2007) The multifunctional nucleolus Nat Rev Mol Cell Biol, 8, 574-585.
71. T. M. Savino, J. Gebrane-Younes, J. De Mey, J. B. Sibarita, D. Hernandez-Verdun (2001) Nucleolar assembly of the rRNA processing machinery in living cells J Cell Biol, 153, 1097-1110.

2. Development of an inhibitor specific for PPM1D phosphatase

2.1. Abstract

PPM1D is a p53-inducible Ser/Thr phosphatase. In cellular responses to genotoxic stress, PPM1D regulates the p53 signaling pathway in a negative feedback manner by dephosphorylating p53 and related factors. Our previous study revealed that overexpression of PPM1D increases the nucleolar number, which is a characteristic of malignant tumors. Overexpression and gene amplification of PPM1D were reported in various cancers including breast cancer, and PPM1D phosphatase activity has been associated with tumorigenesis. Therefore, inhibitors targeting PPM1D may be promising candidates for anticancer agents.

Our laboratory previously developed a potent PPM1D specific inhibitor, SPI-001. In this section, I describe the development of SL-176, a novel PPM1D-specific inhibitor. SL-176 is a simpler structure and size than that of SPI-001. Importantly, SL-176 inhibited PPM1D phosphatase activity to the same degree as SPI-001 despite its smaller structure. SL-176 had only a modest effect on other Ser/Thr phosphatases, including PPM1A, PP1 and PP2A, indicating that SL-176 has high specificity for PPM1D. Kinetics analysis showed that the inhibition manner of SL-176 was a noncompetitive manner. Flow cytometry analysis and cell imaging assay showed SL-176 induced G2/M arrest and apoptosis in MCF7 cells. These results suggested that SL-176 inhibited cancer cell proliferation through specific inhibition of PPM1D. These findings indicate that SL-176 can be a lead compound for anti-cancer chemotherapy. Moreover, SL-176 should be powerful tool for further investigation of the biological functions and mechanisms of PPM1D because of its specificity.

2.2. Introduction

The Ser/Thr phosphatase PPM1D negatively regulates the genotoxic stress response. PPM1D dephosphorylates various proteins, including p53, p38 MAPK, ATM and Chk1/2 (*1-3*). Overexpression of PPM1D is also reported in many types of tumors (*4-8*). Next generation sequencing analysis showed that truncation of the PPM1D C-terminus region is a predisposition factor for breast and ovarian cancer (*9*). Moreover, some studies suggested that PPM1D is a candidate prognosis marker of non-small cell lung cancer, colorectal cancer and gastric cancer (*10-12*). Additionally, gene amplifications of *PPM1D* are frequently observed in neuroblastoma and medulloblastoma (*13-14*). Neuroblastoma and medulloblastoma are known as refractory tumors because of difficulty of surgical treatment. However, effective anti-tumor regents for neuroblastoma and medulloblastoma are not reported. Hence, these observations indicate that PPM1D may be an attractive target for cancer chemotherapy.

Our laboratory previously developed SPI-001, which potently inhibits phosphatase activity of PPM1D (*15*). However, a simpler structure is required for use as a clinical compound for chemotherapy. In general, simpler inhibitors are superior in synthesis, solubility in water and cell membrane penetration. Thus, it is necessary to develop a low molecular weight compound with high inhibitory activity to improve synthesis.

In this study, I have developed SL-176, a novel inhibitor specific for PPM1D. SL-176 potently inhibited PPM1D enzyme in a noncompetitive manner. *In vitro* analysis showed high specificity of SL-176 toward PPM1D.

2.3. Experimental procedures

2.3.1 Expression and purification of human PPM1D catalytic domain

PPM1D 1-420 residues containing catalytic domain was purified as His-tag protein. His-PPM1D(1-420) was expressed in *E.coli* BL21 (DE3) pLysS cells. The cell pellets were lysed in lysis buffer (25 mM HEPES-NaOH pH6.8, 1 M NaCl, 1 mM $MgCl_2$, 10% Glycerol, 0.2% TritionX-100 and 1 mM APMSF) by French press. Affinity purification was carried out with TALON (Clontech, Takara Inc.) and protein was eluted with elution buffer (25 mM HEPES-NaOH pH6.8, 150 mM imidazole, 200 mM NaCl, 1 mM $MgCl_2$, 10% Glycerol, 0.005% TritionX-100). Fractions containing PPM1D(1-420) were further purified, using HiTrap SP FF (GE Healthcare,. England) with ion exchange chromatography start buffer (25 mM HEPES-NaOH pH6.8, 100 mM NaCl, 1 mM $MgCl_2$, 10% Glycerol, 0.005% TritionX-100) and ion exchange chromatography elution buffer (start buffer containing 1 M NaCl). Peak fractions were applied to a Superdex 75 (GE Healthcare, England) column and eluted with size exclusion chromatography elution buffer (25 mM HEPES-NaOH pH6.8, 500 mM NaCl, 1 mM $MgCl_2$, 10% Glycerol, 0.005% TritionX-100). His-PPM1A purified similarly. Protein concentration was measured with image analysis of SDS-PAGE gel.

2.3.2. Synthesis and purification of substrate peptides

All peptide were synthesized Fmoc chemistry using a peptide synthesizer (Applied Biosystems 433A, Foster City, CA). Fmoc amino acids were purchased from Novabiochem (San Diego, CA).The peptides were purified by Vydac C-8 HPLC column (Hesperia, CA) with 0.04% trifluoroacetic acid/water/acetonitrile. The mass of peptide

was confirmed by MALDI mass spectrometry (Applied Biosystems Voyager-DE STR-H, Foster City, CA).

2.3.3. *in vitro* phosphatase assay

Phosphatase activity was assayed by measuring the released free phosphate by BIOMOL GREEN (Enzo life sciences, Farmingdale, NY). All assay carried out in 50 mM Tris-HCl pH7.5, 50 mM NaCl, 30 mM $MgCl_2$, 0.1 mM EGTA, 0.02% 2-mercaptoethanol, 1% DMSO with 2 nM His-PPM1D(1-420), 5 nM His-PPM1A, 1 U/mL PP1 or 1 U/mL PP2A. Substrate sequences were Ac-VEPPLS(P)QETFSD LW-NH_2 (for PPM1D), Ac-TDDE(Nle)T(P)GY(P)VAT -NH_2 (for PPM1A and PP2A) and Ac-WGAKAKKT(P)PKAKK-NH_2 (for PP1). IC_{50} values were calculated by fitting data points with KaleidaGraph4.0 (HULINKS, Japan).PP1 and PP2A were purchased from Biolads (Berkeley, CA) and Promega (Madison, WI) respectively.

2.3.4. Steady-state kinetics assay

Kinetics analysis was performed to analyze inhibition manner of PPM1D inhibitor. Reaction condition was the same with *in vitro* phosphatase assay. Data were fitted to following equation.

$$v = (V_{max} / \alpha') [S] / (\alpha/\alpha' K_m + [S]), \alpha = \alpha' = 1 + [1]/K_i$$

Global fitting was performed with Prism software (Graphpad, CA).

2.3.5. Apoptotic analysis

MCF7 breast cancer cell was obtained from ATCC (Rockville, MD). Cell line was cultured in Dulbecco's modified medium with 10% fetal bovine containing 100 unit/ml

penicillin and 100 μg/ml of streptomycin in humidified atmosphere of 5% CO_2. 2 x 10^4 MCF7 cells were plated onto 3.5 cm cell culture dish and incubated for 24 h and then treated with SL-176. After 24 h from drug treatment, the cells were trypsinized. Trypsinized cells were fixed with 70 % ethanol and stained with PI/RNase Staining Buffer (BD, NJ). Samples were analyzed by Gallios (Beckman coulter, Inc., CA). The data were analyzed with Flowjo (Flowjo, LLC, OR).

2.3.6. The cell cycle analysis

MCF7 cells were plated onto 35 mm dish with 2 ml of medium and incubated for 24 h before drug treatment. After 7 h from drug treatment, the cells were stained with Annexin-V-FLUOS Staining Kit (Roche, Inc.). Samples were analyzed by Biorevo BZ-9000 (Keyence, Inc.). Both Annexin V positive cells and PI negative cells were counted in the images.

2.4. Results

2.4.1 Inhibitory activity of SL-176 toward PPM1D phosphatase

I developed a novel PPM1D inhibitor, namely SL-176, which is an analog of SPI-001 and targets PPM1D phosphatase activity (**Figure 2-1**). SPI-001 has a perhydrophenanthrene ring and two hydrophobic moieties. The molecular weight of SPI-001 is 541.0 and its synthesis requires 24 steps. SL-176 has a decahydronaphthalene ring, two hydrophobic moieties and carboxyl group. The molecular weight of SL-176 is 456.8 and its synthesis requires only 10 steps. Inhibitory activities toward PPM1D were measured by *in vitro* phosphatase assays using His-PPM1D(1-420) and phosphopeptide substrate. SL-176 showed strong PPM1D inhibitory activity at the same level as SPI-001 and GSK2830371, another PPM1D inhibitor, even though its structure is simpler than SPI-001. The IC_{50} value of SL-176 was 110 ± 12.9 nM (**Figure 2-2, Table 2-1**).

2.4.2 Inhibition manner of SL-176

I next analyzed the inhibition manner of SL-176 with kinetics analysis (**Figure 2-3**). Lineweaver-Burk plot analysis was performed with 0, 50, 100 and 150 nM of SL-176. The kinetics analysis data demonstrated that the inhibition manner of SL-176 is via a noncompetitive manner. The K_i value of SL-176 was 228 ± 25 nM. Noncompetitive inhibition means that SL-176 can bind both enzyme and enzyme-substrate complexes, suggesting that inhibition activity of SL-176 does not affect substrate concentrations of PPM1D.

2.4.3. Specificity of SL-176 for PPM1D phosphatase

The specificity of SL-176 inhibition of PPM1D was next analyzed using PPM1A, PP1 and PP2A (**Figure 2-4**). PPM1A is a member of the PPM1 phosphatase family, which has a PPM1 catalytic domain, while PP1 and PP2A belong to different phosphatase families. The catalytic domains of PP1 and PP2A do not show structural similarity with the PPM1 catalytic domain. At 1 μM, the inhibitory activity of SL-176 toward PPM1A was only 11.5%, and SL-176 did not affect PP1 and PP2A phosphatase activity. These results suggest that SL-176 has high specificity toward PPM1D.

2.4.4. Induction of apoptosis by SL-176 in PPM1D overexpressing cells

Our laboratory reported that SL-176 potently represses proliferation of the MCF7 breast cancer cell line in which PPM1D is overexpressed, with an IC_{50} of SL-176 of 7.4 ± 0.72 μM (*16*). I next analyzed the mechanism of cell proliferation repression by SL-176. At high concentrations of SL-176 (20 μM), SL-176 increased the G2/M fraction of the cell cycle and induced apoptosis in MCF7 cells (**Figure 2-5 and 2-6**). These results suggest that SL-176 represses cell cycle proliferation via induction of G2/M cell cycle arrest and apoptosis.

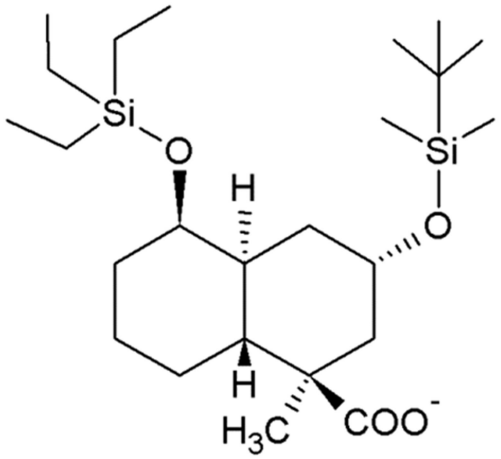

Figure 2-1 Chemical structure of SL-176.

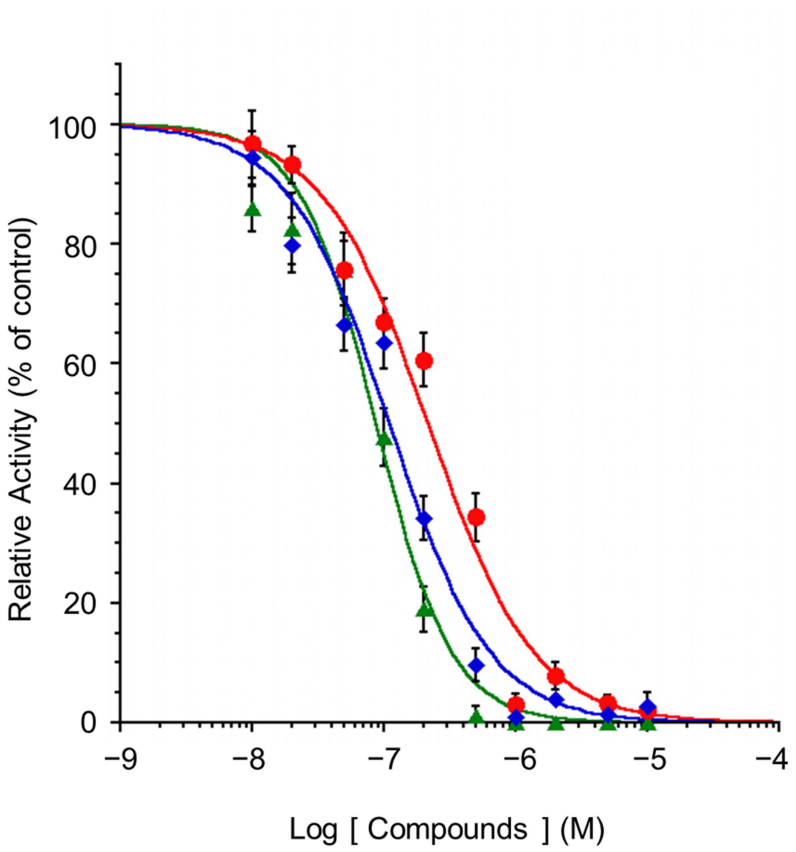

Figure 2-2 Inhibitory activity of SL-176.

Inhibitory activities of SL-176 (circle), SPI-001 (triangle) and GSK2830371 (Rhombus) were analyzed with His-PPM1D(1-420) enzyme. Data represent the mean ± S.D. of 9 points, respectively, from independent experiments.

Table 2-1 IC_{50} value of PPM1D inhibitors.

Inhibitor	IC_{50} (nM)
SL-176	110 ± 12.9
SPI-001	86.9 ± 8.43
GSK2830371	86.3 ± 8.80

Data were calculated by data of figure 2-2. Values of ± were fitting errors.

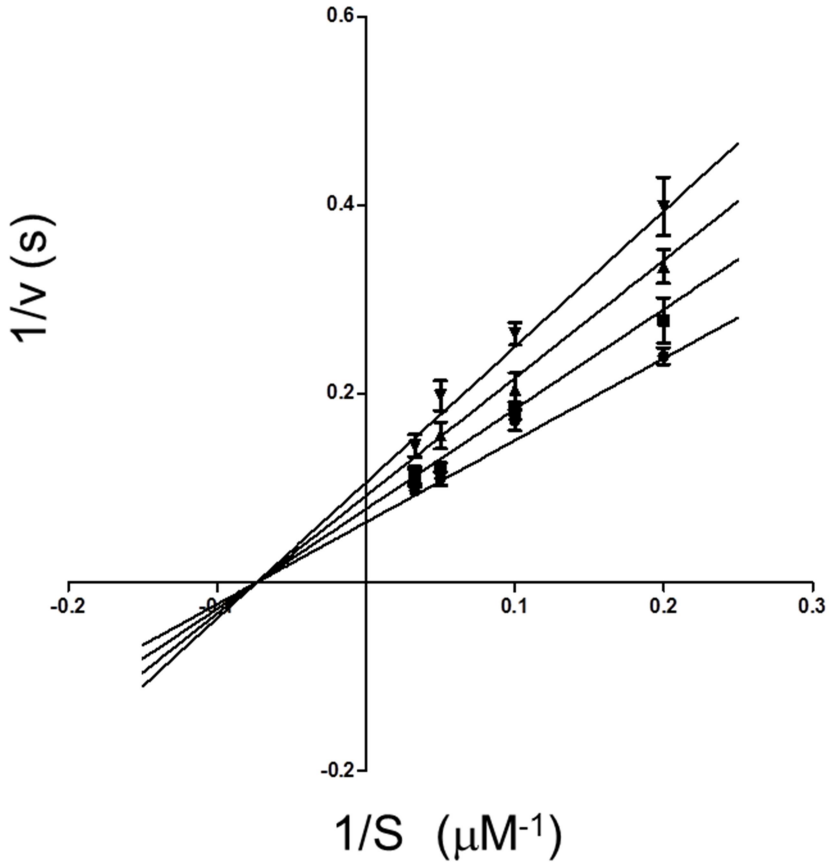

Figure 2-3 Inhibitory manner of SL-176.

Inhibitory manner of SL-176 was analyzed at 0 (circle), 50 (squre), 100 (triangle) and 150 (inverted triangle) nM of SL-176. The K_i value of SL-176 was 228 ± 25 nM. Data represent the mean ± S.D. of 9 points, respectively, from independent experiments.

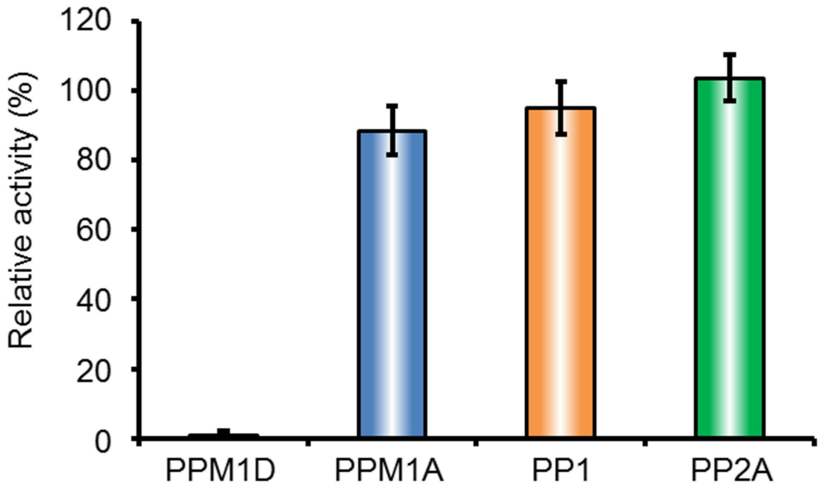

Figure 2-4 Specificity of Sl-176 toward phosphatases.

In 1 μM of SL-176, inhibitory activities were analyzed using PPM1A, PP1 and PP2A phosphatase. Data represent the mean ± S.D. of 3 points, respectively, from independent experiments.

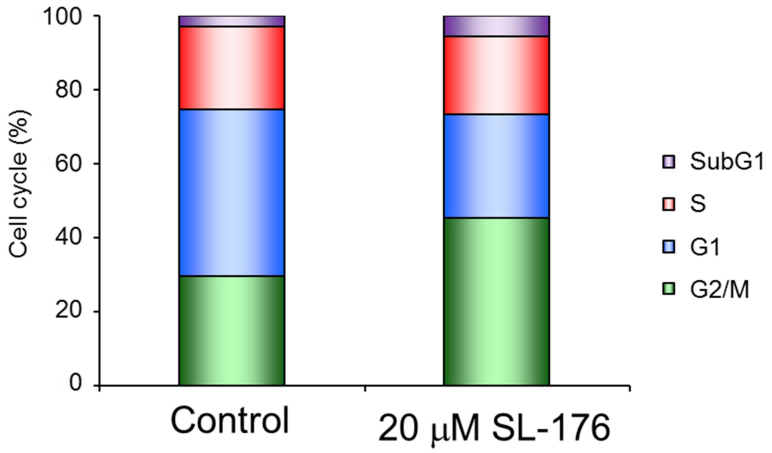

Figure 2-5 Effect of SL-176 on MCF7 cell cycle.

MCF7 was incubated with 20μM SL-176. Representative data were shown in independent 3 experiments.

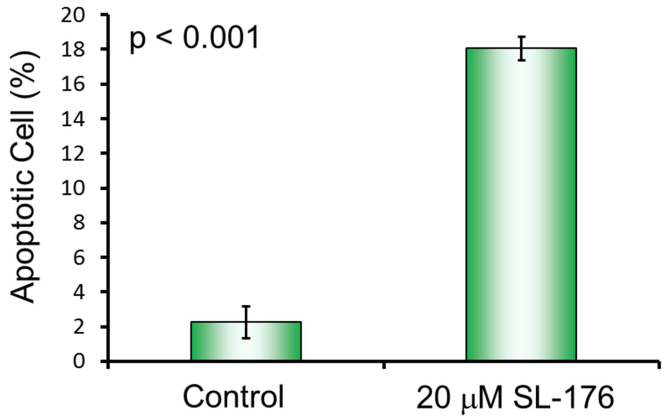

Figure 2-6 Effect of SL-176 on apoptosis.

MCF7 was incubated with 20μM SL-176 in 7 hours. Apoptotic celle were counted by Annexin-V staining. Data represent the mean ± S.D. of 3 points, respectively, from independent experiments.

2.5. Discussion

In this study, I report the development of SL-176 as a PPM1D specific inhibitor. SL-176 showed high specificity toward PPM1D. Our group previously reported SL-176 repression of proliferation of MCF7 human breast cancer cells, in which PPM1D is overexpressed (*16*). SL-176 was more effective than SPI-001 and GSK2830371 on repression of MCF7 cell proliferation. SL-176 activated p53 via inhibition of dephosphorylation on Ser15 of p53, which is a PPM1D target site. The current study also showed that SL-176 induces G2/M arrest and apoptosis, suggesting that SL-176 represses proliferation of MCF7 via G2/M arrest and apoptosis, which are induced by activated p53. Together these results indicate that SL-176 is useful as a lead compound for chemotherapy.

Thus far, two PPM1D inhibitors, CCT007093 and GSK2830371, have been reported as commercially available PPM1D inhibitors (*17-18*). CCT007093 and GSK2830371 have completely different structures from SL-176. Therefore, binding sites of the three inhibitors to PPM1D should be different from each other. Different binding sites suggest that each inhibitor has specific characteristics, such as inhibition mechanisms and conditions. The structural variety of inhibitors provides a diversity of strategies for inhibitor development. Therefore, SL-176 can contribute to the development of more effective PPM1D inhibitors.

2.6. References

1. X. Lu, T. A. Nguyen, L. A. Donehower (2005) Reversal of the ATM/ATR-mediated DNA damage response by the oncogenic phosphatase PPM1D Cell Cycle, 4, 1060-1064.
2. M. Takekawa, M. Adachi, A. Nakahata, I. Nakayama, F. Itoh, H. Tsukuda, Y. Taya, K. Imai (2000) p53-inducible wip1 phosphatase mediates a negative feedback regulation of p38 MAPK-p53 signaling in response to UV radiation EMBO J, 19, 6517-6526.
3. X. Lu, B. Nannenga, L. A. Donehower (2005) PPM1D dephosphorylates Chk1 and p53 and abrogates cell cycle checkpoints Genes Dev, 19, 1162-1174.
4. D. V. Bulavin, O. N. Demidov, S. Saito, P. Kauraniemi, C. Phillips, S. A. Amundson, C. Ambrosino, G. Sauter, A. R. Nebreda, C. W. Anderson, A. Kallioniemi, A. J. Fornace, Jr., E. Appella (2002) Amplification of PPM1D in human tumors abrogates p53 tumor-suppressor activity Nat Genet, 31, 210-215.
5. Z. T. Li, L. Zhang, X. Z. Gao, X. H. Jiang, L. Q. Sun (2013) Expression and significance of the Wip1 proto-oncogene in colorectal cancer Asian Pac J Cancer Prev, 14, 1975-1979.
6. P. Loukopoulos, T. Shibata, H. Katoh, A. Kokubu, M. Sakamoto, K. Yamazaki, T. Kosuge, Y. Kanai, F. Hosoda, I. Imoto, M. Ohki, J. Inazawa, S. Hirohashi (2007) Genome-wide array-based comparative genomic hybridization analysis of pancreatic adenocarcinoma: identification of genetic indicators that predict patient outcome Cancer Sci, 98, 392-400.
7. D. S. Tan, M. B. Lambros, S. Rayter, R. Natrajan, R. Vatcheva, Q. Gao, C. Marchio, F. C. Geyer, K. Savage, S. Parry, K. Fenwick, N. Tamber, A. Mackay, T. Dexter, C. Jameson, W. G. McCluggage, A. Williams, A. Graham, D. Faratian, M. El-Bahrawy, A. J. Paige, H. Gabra, M. E. Gore, M. Zvelebil, C. J. Lord, S. B. Kaye, A. Ashworth, J. S. Reis-Filho (2009) PPM1D is a potential therapeutic target in ovarian clear cell carcinomas Clin Cancer Res, 15, 2269-2280.
8. F. Saito-Ohara, I. Imoto, J. Inoue, H. Hosoi, A. Nakagawara, T. Sugimoto, J. Inazawa (2003) PPM1D is a potential target for 17q gain in neuroblastoma Cancer Res, 63, 1876-1883.
9. E. Ruark, K. Snape, P. Humburg, C. Loveday, I. Bajrami, R. Brough, D. N. Rodrigues, A. Renwick, S. Seal, E. Ramsay, V. Duarte Sdel, M. A. Rivas, M. Warren-Perry, A. Zachariou, A. Campion-Flora, S. Hanks, A. Murray, N. Ansari Pour, J. Douglas, L. Gregory, A. Rimmer, N. M. Walker, T. P. Yang, J. W. Adlard, J. Barwell, J. Berg, A. F. Brady, C. Brewer, G. Brice, C. Chapman, J. Cook, R. Davidson, A. Donaldson, F. Douglas, D. Eccles, D. G. Evans, L. Greenhalgh, A. Henderson, L. Izatt, A. Kumar, F. Lalloo, Z. Miedzybrodzka, P. J. Morrison, J. Paterson, M. Porteous, M. T. Rogers, S. Shanley, L. Walker, M. Gore, R. Houlston, M. A. Brown, M. J. Caufield, P. Deloukas, M. I. McCarthy, J. A. Todd, Breast, C. Ovarian Cancer Susceptibility, C. Wellcome Trust Case Control, C. Turnbull, J. S. Reis-Filho, A. Ashworth, A. C. Antoniou, C. J. Lord, P. Donnelly, N. Rahman (2013) Mosaic PPM1D mutations are associated with predisposition to breast and ovarian cancer Nature, 493, 406-410.

10. H. Yang, X. Y. Gao, P. Li, T. S. Jiang (2015) PPM1D overexpression predicts poor prognosis in non-small cell lung cancer Tumour Biol, 36, 2179-2184.
11. T. S. Peng, Y. H. He, T. Nie, X. D. Hu, H. Y. Lu, J. Yi, Y. F. Shuai, M. Luo (2014) PPM1D is a prognostic marker and therapeutic target in colorectal cancer Exp Ther Med, 8, 430-434.
12. D. Ma, C. J. Zhang, Z. L. Chen, H. Yang (2014) Prognostic value of PPM1D in 800 gastric cancer patients Mol Med Rep, 10, 191-194.
13. M. C. Buss, M. Remke, J. Lee, K. Gandhi, M. J. Schniederjan, M. Kool, P. A. Northcott, S. M. Pfister, M. D. Taylor, R. C. Castellino (2015) The WIP1 oncogene promotes progression and invasion of aggressive medulloblastoma variants Oncogene, 34, 1126-1140.
14. M. Richter, T. Dayaram, A. G. Gilmartin, G. Ganji, S. K. Pemmasani, H. Van Der Key, J. M. Shohet, L. A. Donehower, R. Kumar (2015) WIP1 phosphatase as a potential therapeutic target in neuroblastoma PLoS One, 10, e0115635.
15. H. Yagi, Y. Chuman, Y. Kozakai, T. Imagawa, Y. Takahashi, F. Yoshimura, K. Tanino, K. Sakaguchi (2012) A small molecule inhibitor of p53-inducible protein phosphatase PPM1D Bioorg Med Chem Lett, 22, 729-732.
16. S. Ogasawara, Y. Kiyota, Y. Chuman, A. Kowata, F. Yoshimura, K. Tanino, R. Kamada, K. Sakaguchi (2015) Novel inhibitors targeting PPM1D phosphatase potently suppress cancer cell proliferation Bioorg Med Chem, 23, 6246-6249.
17. S. Rayter, R. Elliott, J. Travers, M. G. Rowlands, T. B. Richardson, K. Boxall, K. Jones, S. Linardopoulos, P. Workman, W. Aherne, C. J. Lord, A. Ashworth (2008) A chemical inhibitor of PPM1D that selectively kills cells overexpressing PPM1D Oncogene, 27, 1036-1044.
18. A. G. Gilmartin, T. H. Faitg, M. Richter, A. Groy, M. A. Seefeld, M. G. Darcy, X. Peng, K. Federowicz, J. Yang, S. Y. Zhang, E. Minthorn, J. P. Jaworski, M. Schaber, S. Martens, D. E. McNulty, R. H. Sinnamon, H. Zhang, R. B. Kirkpatrick, N. Nevins, G. Cui, B. Pietrak, E. Diaz, A. Jones, M. Brandt, B. Schwartz, D. A. Heerding, R. Kumar (2014) Allosteric Wip1 phosphatase inhibition through flap-subdomain interaction Nat Chem Biol, 10, 181-187.

3. Increased micronucleolus formation by PPM1D correlated with nucleolar number

3.1. Abstract

The nucleolus is a structure within the nucleus. The nucleolus regulates ribosomal biosynthesis, cell cycle regulation, DNA damage response and mRNA processing. In various tumors, abnormal nucleolar morphology is reported. Previous our study revealed that overexpression of PPM1D, a PPM1 type Ser/ Thr phosphatase, induces the nucleolar number via nucleolar protein NPM which is involved in ribosomal biosynthesis and histone. The CDC25C-CDK1-PLK1 pathway is activated by PPM1D, and activated CDK1 and PLK1 phosphorylate Thr199 and Ser4 in NPM, respectively. Structural analysis revealed that NPM forms decamers, and decamer formation is required for DNA and histone interaction. However, the relationship of oligomerization and biological function of NPM is unclear.

In this study, I found a NPM foci, which is named as micronucleolus, in the nucleus of PPM1D overexpressed cell. PPM1D inhibitor SL-176 demonstrated that activity of PPM1D increased micronucleolar formation. I showed that phosphorylation of Ser4 and Thr199 in NPM, which are regulated by PPM1D, affected NPM oligomer formation. Phosphomimic mutants of NPM demonstrated that phosphorylation of Ser4 and Thr 199 destabilizes NPM decamers. These results suggest that PPM1D destabilizes NPM via induced phosphorylation of Ser4 and Thr 199 of NPM by CDK1 and PLK1 kinase. The destabilization of NPM decamer

3.2. Introduction

The nucleolus is a structure in the nucleus that regulates ribosomal synthesis. In many types of tumors, increases of nucleolar number, nucleolar hypertrophy and abnormal shape are observed (*1*-*2*). Morphology of the nucleolus is one of cytodiagnostic criteria in tumor malignancy (*3*). Previous studies reported that the nucleolar assembly and disassembly are cell cycle-dependent (*4*). However, the molecular mechanism underlying the increase of nucleolar number in cancer has remained unclear. Our laboratory has reported that protein phosphatase PPM1D increases nucleolar number via phosphorylation of the nucleolar protein NPM (*5*). Overexpressed PPM1D induces activation of CDC25C-CDK1-PLK1 pathway. Activated CDK1-cyclin B and PLK1 phosphorylate Ser4 and Thr199 of NPM, respectively. As a result, phosphorylated NPM increases nucleolar number in cancer cells.

The nucleolus is disassembled in the mitotic phase. Nucleolar proteins, including NPM, translocate to the cytoplasm and/or chromatin. The nucleoli are then formed centering on nucleolus organizer regions (NORs) in early G1 phase, and proteins that compose the granular component (GC) and dense fibrillar component (DFG) associate into pre-nucleolus body (PNB) apart from NORs (*6*). During the progression of G1 phase, NORs fuse and increase in size, while PNBs increase in size and then disappear. PNB do not fuse with NORs or each other (*4*). PNB-associated factors then dissociate from PNB and are recruited to NORs.

In this study, I showed that phosphorylation of Ser4 and Thr199 in NPM by PPM1D destabilizes decamer formation of NPM. The destabilization of NPM decamer induced formation of micornucleolus and increase of the nucleolar number.

3.3. Experimental procedures

3.3.1. Cell culture

MCF7 breast cancer cell and H1299 carcinoma non-small cell were obtained from ATCC (Rockville, MD). Cell line was cultured in Dulbecco's modified medium with 10% fetal bovine containing 100 unit/ml penicillin and 100 μg/ml of streptomycin in humidified atmosphere of 5% CO_2. For knock down of endogenous PPM1D and NPM, siRNA was transfected with Lipofectamine 2000 (Invitrogen, Carlsbad, CA). siRNA sequence for PPM1D and NPM are followed: 5'-GAAGUGGACAAUCAGGGAA ACUUUA-3' and 5'-AUAUAUAGACCCUGAAGAUCUCGCG-3', respectively. The target specific siRNA duplexes were designed with Invitorgen BLOCK-iTTM RNAi Designer. PMD-9, PMD-12 and PMD-F4 which are PPM1D expressed stable cell line are derived from H1299. HA-tagged NPM mutants are prepared as previously described (*5*).

3.3.2. Antibodies

Rabbit poly clonal antibody specific for PPM1D are generated as previously described (*7*). Other antibodies are followed: Mouse monoclonal anti-NPM (FC-61991, Invitrogen), a rabbit polyclonal anti-HA (Y-11, Santa Cruz Biotechnology), a mouse monoclonal anti-actin (Ab-1, Calbiochem), an anti-mouse IgG HRP-linked antibody (GE healthcare, England), an anti-rabbit IgG HRP-linked antibody (Cell signaling), an anti-mouse IgG Alexa Fluor488 goat anti-mouse IgG (Invitrogen) and anti-rabbit IgG Alexa Fluor568 goat IgG (Invitrogen).

3.3.3. Western blotting analysis

Cells were harvested with 1x sample buffer (50 mM Tris-HCl, pH6.8, 10% Glycerol, 2% SDS, 6% 2-mercaptoethanol). Equivalent amount of total cellular protein were separated with SDS-PAGE. Proteins were transferred to polyvinylidene difluoride membranes from SDS-PAGE gel. Proteins were detected with antibody descried above by enhanced chemiluminescence.

3.3.4. Immunofluorescence studies and quantification

Cell was fixed with 3.5% formalin/PBS at 15 min. After washing, cell was treated with 0.2% TritonX-100/PBS. In order to block non-specific signal, cell was incubated with 10% FBS/PBS. Immunostaining was performed following antibodies: mouse polyclonal anti-HA (Roche, Basel, Switzerland) and Alexa Fluor568 goat anti-Rabbit IgG (Invitrogen, Carlsbad, CA). Nucleus of cell was detected with DAPI. For quantification of nucleolus number, samples were analyzed by Biorevo BZ-9000 (Keyence, Japan). Nucleolus number was counted manually.

3.3.5. Expression and purification of NPM mutants

NPM mutants were purified as His-tag protein. NPM mutants were expressed in *E.coli* BL21 (DE3) pLysS cells with pCold I vector (Takara, Japan). Protein expression was induced with 16^{o}C and 1 mM IPTG. The cell pellets were lysed in lysis buffer (50 mM Na phosphate buffer pH7.5, 500 mM NaCl, 1 mM 2-mercaptoethanol, 10% Glycerol, 0.2% TritionX-100) by French press. Affinity purification was carried out with TALON (Clontech, Takara, Japan) and protein was eluted with elution buffer (50 mM Na phosphate buffer pH7.5, 500 mM NaCl, 150 mM imidazole, 1 mM

2-mercaptoethanol, 10% Glycerol,). Fractions containing NPM were dialyzed with dialysis buffer (50 mM Na phosphate buffer pH7.5, 500 mM NaCl). The concentration of NPM is calculated with ε = 16960 at 280 nm.

3.3.6. Size exclusion chromatography analysis

NPM mutants were analyzed with TOSOH TSK-GEL G3000S_{WXL} (TOSOH, Japan). Elution buffer NPM was 50 mM Na phosphate buffer pH7.5 containing 500 mM NaCl.

3.3.7. Circular dichroism spectrum analysis

NPM mutants were analyzed with J-805 circular dichroism spectrum meter (JASCO, Japan). Buffer condition was 50 mM Na phosphate buffer pH7.5 containing 500 mM NaCl at 4 ^{o}C. Sample concentration was 2 μM.

3.3.8. Cell cycle analysis

Cells were plated onto 3.5 cm cell culture dish and incubated for 48 h. After 48 h from plating, the cells were trypsinized. Trypsinized cells were fixed with 70 % ethanol and stained with PI/RNase Staining Buffer (BD, NJ). Samples were analyzed by Gallios (Beckman coulter, Inc., CA). The data were analyzed with Flowjo (Flowjo, LLC, OR)

3.4. Results

3.4.1. Formation of the micronucleolus in PPM1D overexpressing cells

NPM is a nucleolar protein localized in the nucleus and the nucleolus. In early G1 phase, NPM is located in PNBs and NORs. PNB-like NPM foci are observed in the nucleus of the MCF7 cell line in which PPM1D is overexpressing cell (**Figure 3-1, Table 3-1**). Our laboratory named PNB-like NPM foci "the micronucleoli", and we found that 3.9% of MCF7 cells contain these micronucleoli. PNBs are observed in early G1 cells. After mitotic phase, the cells which have PNB are pair. Unlike PNB, the cells which have the micronucleoli are not pair. Notably, we found that MCF7 cells transfected with PPM1D siRNA results in only 1.1% of MCF7 cells with micronucleoli. (**Figure 3-2, Table 3-2**). I next generated H1299 PMD-9 and PMD-12 clones that stably express HA-tagged PPM1D and PMD-F4 clones that stably express $Flag_5$-tagged PPM1D (**Figure 3-3, Table 3-2**). Comparing PPM1D expression levels and percentages of micronucleoli, I found that PPM1D expression level showed a positive correlation with the percentage of micronucleoli. In addition, the cell cycle changes of each stable line did not relate to the increase of the nucleolar number and formation of micronucleoli (**Figure 3-4**).

3.4.2. Repression of micronucleoli and nucleoli number by SL-176

SL-176 treatment reduced the percentages of micronucleoli in PPM1D overexpressing stable cell lines but not in H1299 parental cells (**Table 3-3**). This suggests that PPM1D phosphatase activity is associated with micronucleoli formation.

3.4.3. Effects of NPM Ser4 and Thr199 phosphorylation on micronucleoli formation

We next generated a panel of mutants, including HA-NPM S4A, S4D, T199A and T199E. Ala mutants were used as a non-phosphorylated mutant, and Asp and Glu residues were mimics of phosphorylated Ser and Thr. HA-tagged NPM and its mutant were expressed in MCF7 cells in which PPM1D overexpressed and that were transfected with siRNA for knockdown of endogenous NPM. In our previous study, the nucleolar numbers of MCF7 cells that expressed HA-NPM S4A and HA-NPM T199A were decreased compared with MCF7 cells that expressed HA-NPM (*5*). In cells in which HA-mutant highly expressed, micronucleoli were increased comparing with intact MCF7 cell **(Figure 3-5, Table 3-3**). The percentages of cells with micronucleoli were the same among HA-NPM WT, S4A, S4D and T199E expressing cells. Interestingly, only the HA-T199A mutant showed a decreased percentage of cells with micronucleoli, to 46.7%. These findings suggest that PPM1D and phosphorylation of Thr199 affect micronucleoli formation and that PPM1D activity may be involve in micronucleoli formation.

3.4.4. Effects of NPM Ser4 and Thr199 phosphorylation on its oligomerization

Structural analysis showed that NPM forms pentamers and decamers in water. Formation of decamers, which are dimers of pentamers, is required for the interaction of NPM family and histone (*8*). To analyze the effects of phosphorylation of Ser4 and Thr199 in NPM on oligomerization, size exclusion analysis was performed. His-NPM WT, S4D, T199D and S4D/T199E mutants were expressed in *E. coli* and purified with His-affinity chromatography. SDS-PAGE analysis showed that purified NPM mutants

were highly pure (**Figure 3-6**). The results confirmed that His-NPM WT strongly formed decamers (**Figure 3-7**). Only decamer and pentamer peaks with His-NPM WT were observed but not monomer peaks. Surprisingly, S4D and T199E mutants showed weak decamer peaks, compared with WT. The S4D/T199E mutant mainly formed pentamers.

Next, circular dichroism spectra analysis was performed. WT, S4D and T199E mutants showed almost the same spectra (**Figure 3-8**). However the spectrum of the S4D/T199E mutant was different from WT. The spectra change suggested that the random coil structure of the S4D/T199E mutant was increased. These results strongly suggest that phosphorylation of Ser4 and Thr199 destabilizes decamers of NPM, especially dual phosphorylation.

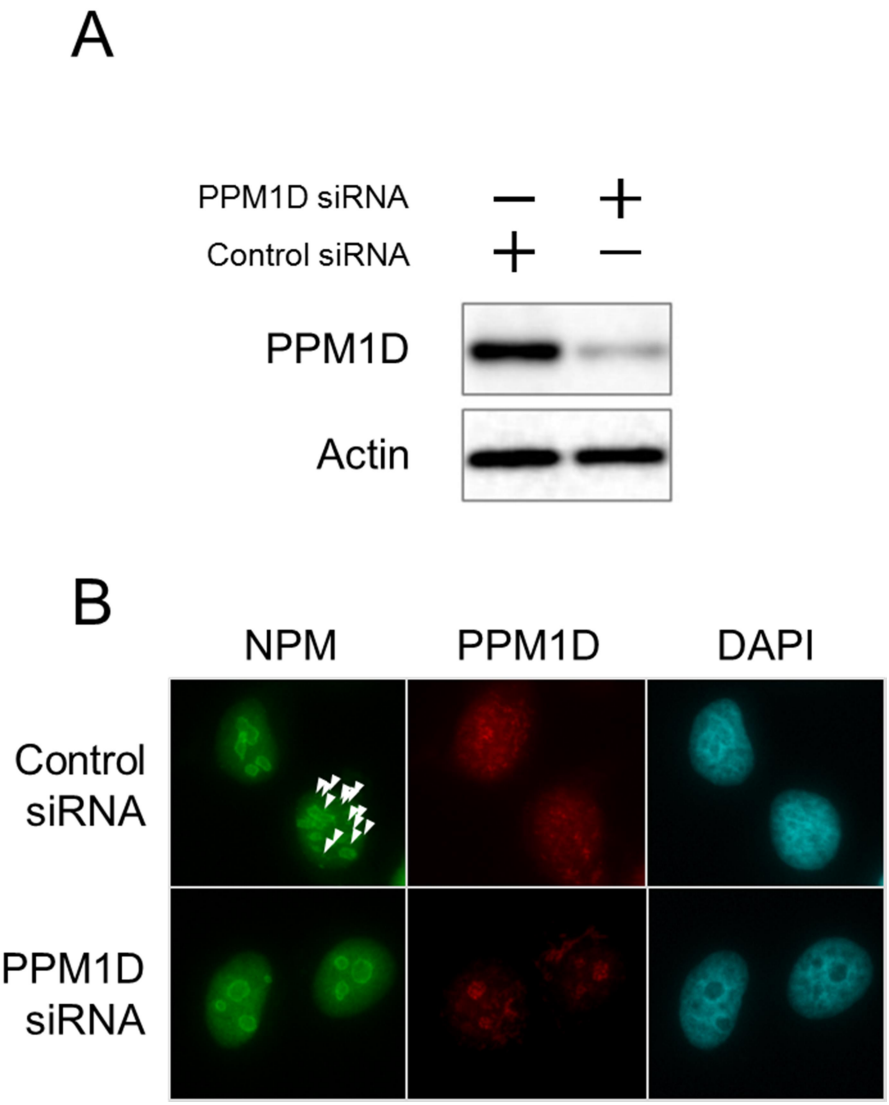

Figure 3-1 the micronucleolus of MCF7

A) Knock down of endogenous PPM1D in MCF7 cell. Actin was used for loading control. B) the micronucleolus in MCF7 cell. White arrow head is the cell which has micronucleolus.

Table 3-1 Percentages of cells which have micronucleolus.

siRNA	Micro-nucleolus (%)	Number of Nucleoli	n
Control	3.9	4.4 ± 0.05	698
PPM1D	1.1	3.7 ± 0.05	714

Data were analyzed by counting the cells which have the micronucleolus. Total cell numbers were 698 and 714 in MCF7 treated with control siRNA and siRNA specific for PPM1D, respectively. Error were SE.

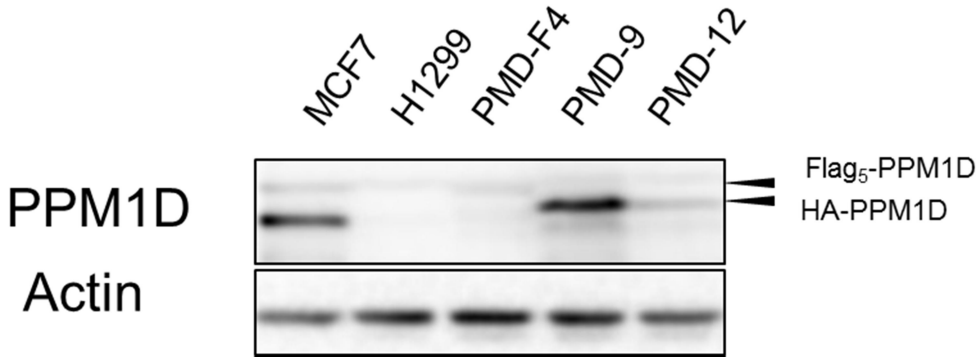

Figure 3-2 Expression level of PPM1D in stable clones

$Flag_5$ tagged PPM1D was expressed in H1299 PMD-F4. H1299 PMD-9 and H1299 PMD-12 expressed HA tagged PPM1D. Actin was used for loading control.

Table 3-2 Percentages of cells which have micronucleolus

PPM1D Level (% of MCF7)	Clone	Micro-nucleolus (%)	Number of Nucleoli	n
4	H1299	2.9	3.8 ± 0.1	722
80*	PMD-9	7.4	5.1 ± 0.1*	743
13*	PMD-12	5.4	4.4 ± 0.1*	592
13	PMD-F4	5.9	4.1 ± 0.1	743

Data were analyzed by counting the cells which have the micronucleolus. Total cell numbers were 319, 253, 717 and 801 in H1299, H1299 PMD-F4, H1299 PMD-9 and H1299 PMD-12, respectively. Error of the nucleolar numbers were SE.* Data are referred from Kozakai. *et.al* (*5*).

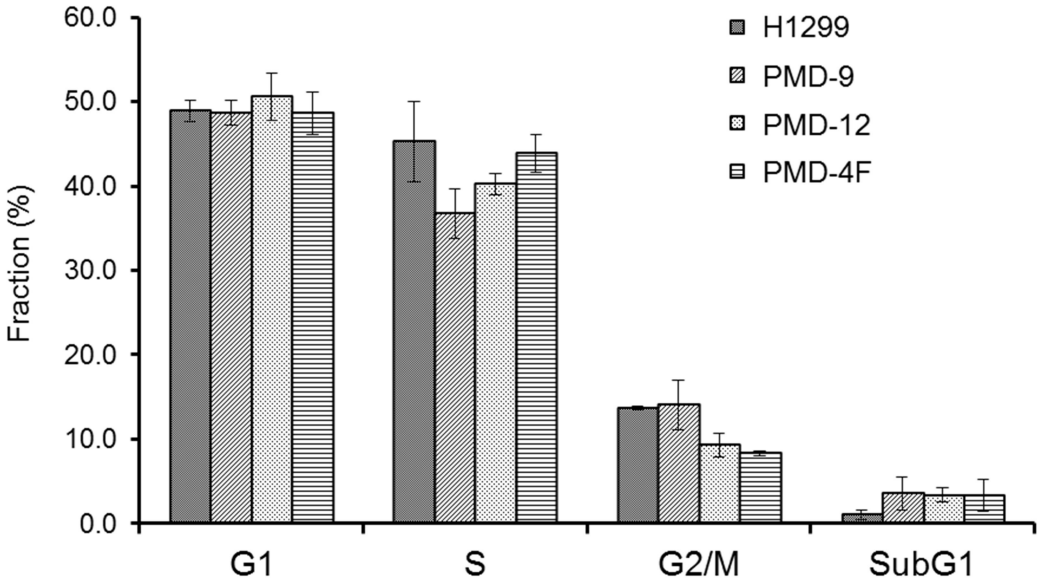

Figure 3-3 Cell cycle of H1299 and PPM1D expressed stable clones

The cell cycle of H1299 PMD-SubP1-F10 and H1299 PMD-SubP2-F12 was analyzed with flow cytometry. Data represent the mean ± S.D. of 3 independent experiments.

Table 3-3 Repression of micronucleolus in H1299 clones by SL-176

PPM1D Level (% of MCF7)	Clone	Treatment	Micro-nucleolus (%)	Number of Nucleoli	n
4	H1299	Vehicle	3.0	3.7 ± 0.1	823
		SL-176	2.6	3.8 ± 0.2	906
80	PMD-9	Vehicle	6.8	5.2 ± 0.2	615
		SL-176	3.6	4.6 ± 0.2	549
13	PMD-12	Vehicle	5.5	4.2 ± 0.2	532
		SL-176	3.4	4.0 ± 0.1	412
13	PMD-F4	Vehicle	5.7	4.2 ± 0.1	846
		SL-176	3.3	3.9 ± 0.1	810

Data were analyzed by counting the cells which have the micronucleolus. Total cell numbers were shown on table. Concentration of SL-176 was 2 μM.

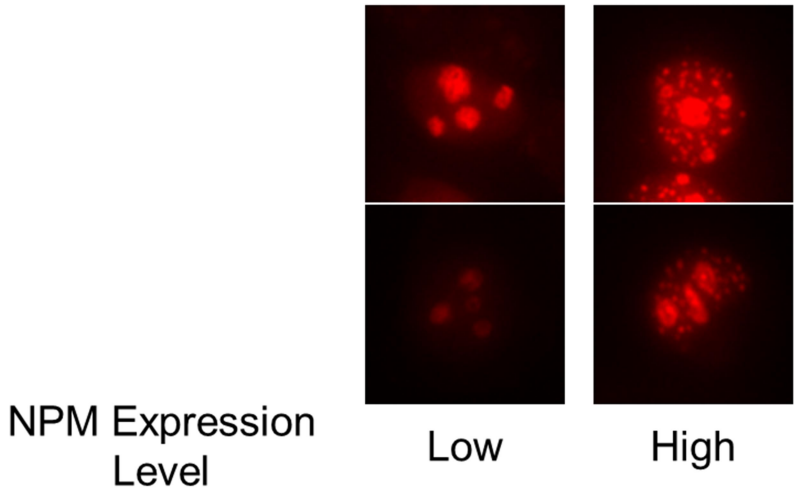

Figure 3-4 Localization of NPM mutants and the micronucleolus in MCF7

The micronucleolus in MCF7 expressed NPM mutant. HA-NPM WT was shown as sexample. In cell which is high expression level of NPM mutant, the micronucleoli were frequently observed.

Table 3-4 Percentages of cells which have micronucleolus in MCF7 expressed NPM mutants

HA-NPM	Micro-nucleolus (%)	n
WT	56.8	595
S4A	60.2	416
S4D	62.6	395
T199A	46.7	703
T199E	59.5	499

Data were analyzed by counting the cells which have the micronucleolus. Total cell numbers were 595, 416, 395, 703 and 499.

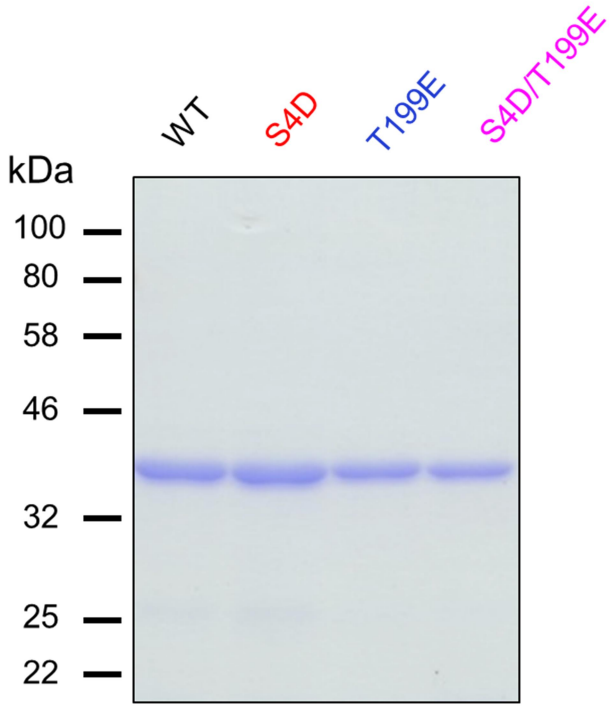

Figure 3-5 SDS-PAGE of His-NPM WT, S4D, T199E and S4D/T199E

Protein was detected with CBB staining.

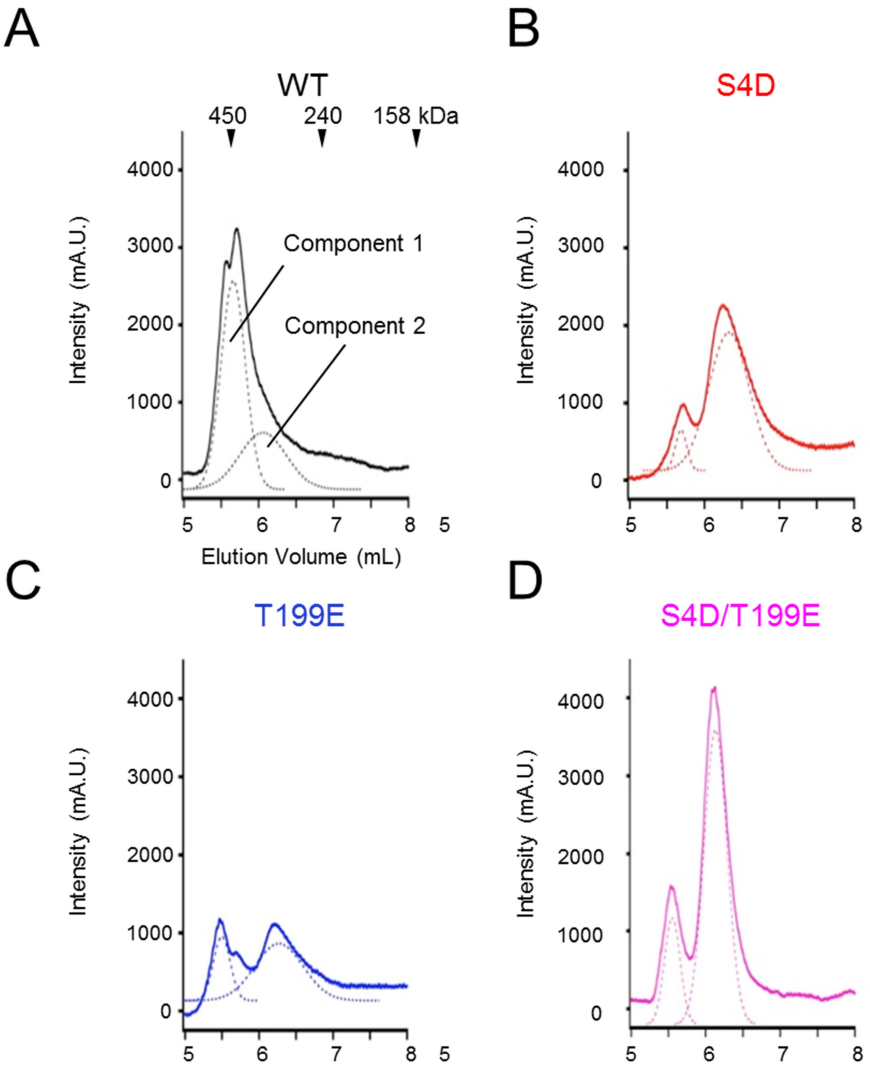

Figure 3-6 SEC analysis of His-NPM WT, S4D, T199E and S4D/T199E

It was reported NPM forms pentamer and decamer. Therefore SEC peaks were deconvoluted as two peaks. Each panel is A)HA-NPM WT, B)HA-NPM S4D, C)HA-NPM T199E, D)HA-NPM S4D/T199E.

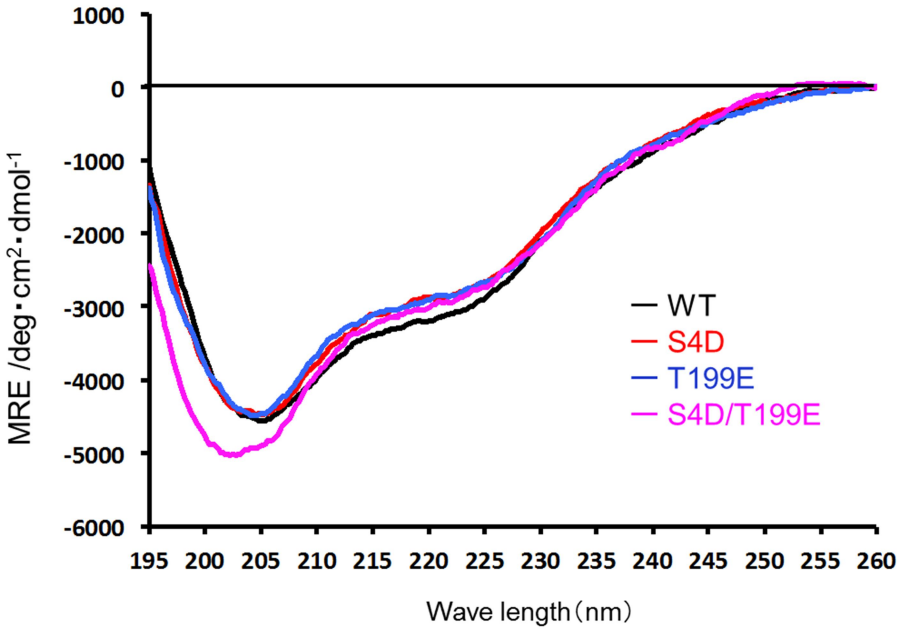

Figure 3-7 CD spectra of His-NPM WT, S4D, T199E and S4D/T199E

CD Spectra were performed at 4°C.

3.5. Discussion

Our previous report showed that knockdown of PPM1D induced a decrease of nucleolar number in MCF7 cells (*5*). Moreover, we demonstrated that PPM1D activity was associated with nucleolar number. In this study, the micronucleolar formation was also decreased by PPM1D knockdown. The PNB forms only during early G1 phase (*4*). Our previous study showed that PPM1D knockdown does not affect cell cycle progression (*5*). In addition, I also demonstrated that the cell cycle does not correlate with the nucleolar number and the micronucleoli formation in this study. Hence, the micronucleoli are qualitatively different from PNB, which is dependent on the cell cycle status. Moreover, PPM1D siRNA treatment and SL-176 demonstrated that PPM1D activity is associated with micronucleolar formation.

The phosphorylation mimic mutant of NPM demonstrated that Ser4 and Thr199 phosphorylation sites affect NPM oligomerization. The NPM phosphomimic showed decreased stability of decamers. Formation of decamer is required for the interaction of histone and DNA with NPM (*6, 8*). However, the relationship between decamer formation and function of NPM are still unclear.

In this study, I examined also micronucleoli. The micronucleoli share a similar structure with PNBs. I propose a hypothesis by which phosphorylated NPM on Ser4 and Thr199 prevents formation of the nucleolus and PNBs. PNBs are formed in early G1 phase (**Figure 3-8**). After the mitotic phase, DG-associated factors, including NPM, are recruited at pre-rRNA, which is maintained from G2 phase. pre-rRNA does not mature in M phase. The main function of PNB is to mature pre-rRNA in early G1 in which nucleolar function is still not recover (*9*). PNB assumes a maturation process of pre-rRNA in early G1 instead of the nucleolus. After maturation of pre-rRNA, PNB

disassembles and incorporates into the nucleolus (*9*). Importantly, PNBs do not fuse with each other during the PNB growth process (*6*). Additionally, PNB also do not fuse into the pre-nucleolus (*4*). PPM1D overexpression enhances Ser4 and Thr199 phosphorylation of NPM and increases the micronucleolar formation. MCF7 cells that stably express HA-NPM T199A demonstrated that phosphorylation of Thr199 positively affects micronucleolar formation. *In vitro* analysis showed that non-phosphorylated NPM forms stable decamers. In addition, phosphorylation of NPM Thr199 decreased ribosomal biosynthesis and inhibited the binding between NPM and histone (*10*). Taken together, destabilization of NPM decamers by phosphorylation, which is regulated by PPM1D, should affect formation of the nucleolus and induce micornucleolus and increase of nucleolar number.

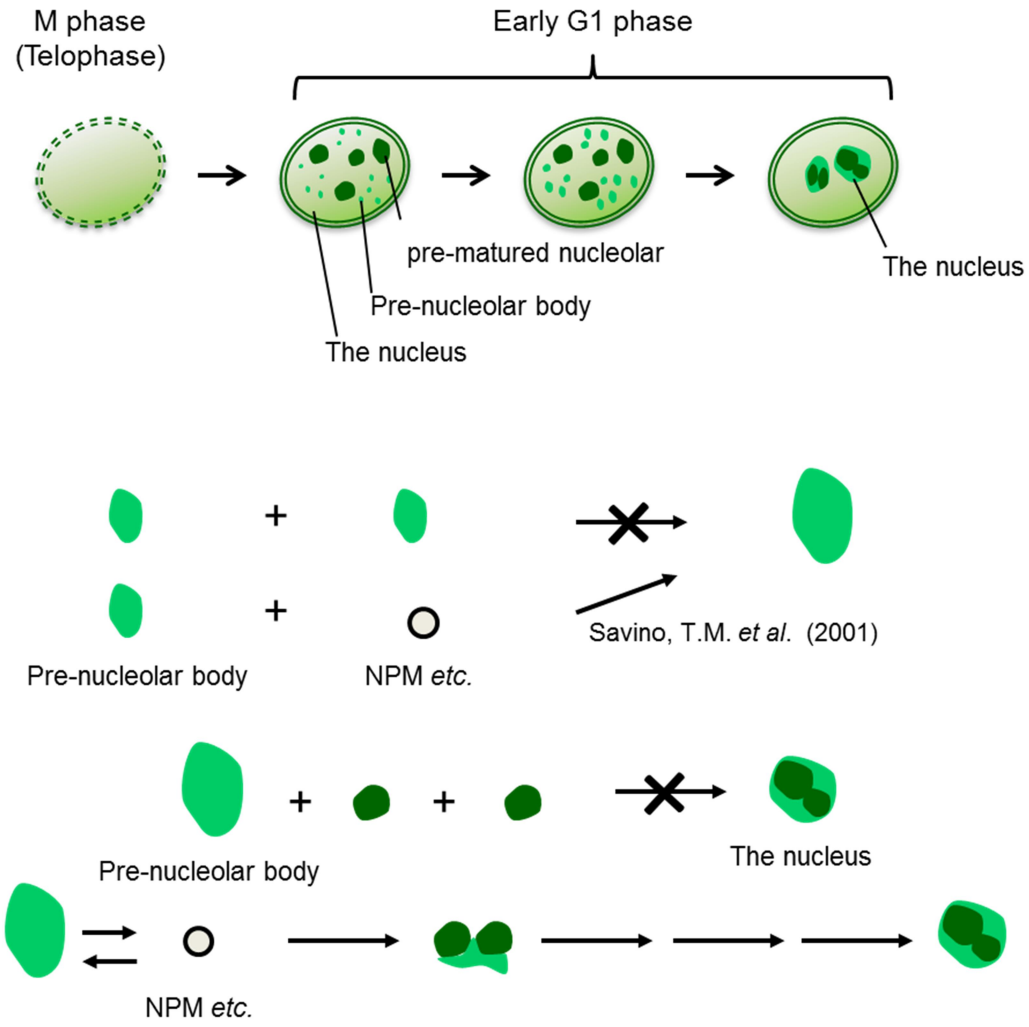

Savino, T.M. *et al.* (2001) and Daniele H.V. *et al.* (2011)

Figure 3-8 Formation of pre-nucleolar body and the nucleolus

Savino T.M. *et al* showed that pre-nucleolar body does not fuse in its grown process (*6*). In the nucleolar formation, pre-nucleolar body and pre-matured nucleolus also do not fuse (*4*).

3.6. References

1. D. Ruggero, P. P. Pandolfi (2003) Does the ribosome translate cancer? Nat Rev Cancer, 3, 179-192.
2. M. Derenzini, L. Montanaro, D. Trere (2009) What the nucleolus says to a tumour pathologist Histopathology, 54, 753-762.
3. D. Ruggero (2012) Revisiting the nucleolus: from marker to dynamic integrator of cancer signaling Sci Signal, 5, pe38.
4. D. Hernandez-Verdun (2011) Assembly and disassembly of the nucleolus during the cell cycle Nucleus, 2, 189-194.
5. Y. Kozakai, R. Kamada, J. Furuta, Y. Kiyota, Y. Chuman, K. Sakaguchi (2016) PPM1D controls nucleolar formation by up-regulating phosphorylation of nucleophosmin Sci Rep, 6, 33272.
6. T. M. Savino, J. Gebrane-Younes, J. De Mey, J. B. Sibarita, D. Hernandez-Verdun (2001) Nucleolar assembly of the rRNA processing machinery in living cells J Cell Biol, 153, 1097-1110.
7. Y. Chuman, W. Kurihashi, Y. Mizukami, T. Nashimoto, H. Yagi, K. Sakaguchi (2009) PPM1D430, a novel alternative splicing variant of the human PPM1D, can dephosphorylate p53 and exhibits specific tissue expression J Biochem, 145, 1-12.
8. O. Platonova, I. V. Akey, J. F. Head, C. W. Akey (2011) Crystal structure and function of human nucleoplasmin (npm2): a histone chaperone in oocytes and embryos Biochemistry, 50, 8078-8089.
9. C. Carron, S. Balor, F. Delavoie, C. Plisson-Chastang, M. Faubladier, P. E. Gleizes, M. F. O'Donohue (2012) Post-mitotic dynamics of pre-nucleolar bodies is driven by pre-rRNA processing J Cell Sci, 125, 4532-4542.
10. M. Hisaoka, S. Ueshima, K. Murano, K. Nagata, M. Okuwaki (2010) Regulation of nucleolar chromatin by B23/nucleophosmin jointly depends upon its RNA binding activity and transcription factor UBF Mol Cell Biol, 30, 4952-4964.

4. Regulation of PPM1D by its specific region P-loop

4.1. Abstract

PPM1D, a PPM1 type Ser/ Thr phosphatase, is overexpressed in various tumors and is likely involved in tumorigenesis. Our laboratory has proposed a novel tumorigenesis mechanism by overexpression of PPM1D via NPM. Overexpression of PPM1D induces the nucleolar number. Increase of nucleolar number is observed in malignant tumors. It is suggested that abnormal regulation of PPM1D involved in tumorigenesis. The catalytic domain of PPM1D is conserved among PPM1 family members. However regulation mechanisms of PPM1D are still unclear. Each family member also contains unique regions, which should be involved in isoform-specific regulation. PPM1D contains a Pro-rich loop (P-loop) as a specific region. These specific regions should be involved in isoform specific regulation.

In this study, I identified the P-loop in PPM1D as a regulatory region for the nucleolar number. Substitution of the P-loop increased the nucleolar number. The effects of P-loop substitution were repressed by SL-176, which is a PPM1D specific inhibitor. *In vitro* analysis suggested that PPM1D forms oligomers. Oligomerization of PPM1D decreased PPM1D phosphatase activity. Those data proposed a novel regulation mechanism of PPM1D that P-loop negatively regulates PPM1D phosphatase activity via oligomerization.

4.2. Introduction

PPM1D (also known as PP2Cδ and Wip1) is a PPM1 type Ser/Thr phosphatase. Overexpression of PPM1D and amplification of *PPM1D* gene are reported in various types of tumors (*1-5*). Previous reports suggested that abnormal upregulation of PPM1D is related to tumorigenesis (*6*). PPM1D belong to the PPM1 family of phosphatases, which share a conserved catalytic domain structure (*7*). However, each isoform also contains unique regions between conserved regions and/or in the N/C terminus (*8*). PPM1D has Pro-rich region, named the P-loop, as a unique region in the catalytic domain. Pro-rich sequences are protein-interaction sequences in various proteins (*9-10*). These unique regions should have a function for isoform specific regulation.

Our group have demonstrated that overexpression of PPM1D induces increase of the nucleolar number. In formation of nucleolus, pre-mature nucleolus is formed in early G1 phase. Maturation process of the nucleolus should be regulated for normal morphology of the nucleolus. Regulation factors of formation of the nucleolus are not still clarified.

In this study, I showed that the P-loop of PPM1D serves as a regulatory region for NPM decamer formation. Substitution of P-loop increases the nucleolar number and the micronucleolar formation, suggesting P-loop negatively regulates PPM1D.

4.3. Experimental procedures

4.3.1. Plasmid construction

Substitution mutant of P-loop are generated with followed strategy. Frist PCR was performed with forward primer (5'-CTTTCCTGCGTTATCCCCTG-3', 5'-GAACCGAGTGGATCCTCCGTGGCCTTT-3', 5'-GAACCGAGTGGATGCTGCC GCCGCCGT-3') and reverse primer (5'-TCCACTCGGTTCGGGCTCCACAAC-3', 5'-GAGGTTTTCACCGTCATC-3'). Second PCR was carried out with first PCR fragments. Using primers of first PCR, third PCR was performed. Expression vectors were used with phCMV2 (Gene Therapy Systems, Inc., San Diego, CA) and pCold I (Takara, Japan) for human cell and E.coli, respectively.

4.3.2. Expression and purification of human PPM1D catalytic domain

Purification methods of His-PPM1D(1-420) are described in chapter 2. For purification of SubP1 mutant, I modified followed buffer: lysis buffer (25 mM HEPES-NaOH pH7.5, 1 M NaCl, 1 mM $MgCl_2$, 10% Glycerol, 0.2% TritionX-100 and 1 mM APMSF), elution buffer (25 mM HEPES-NaOH pH7.5, 150 mM imidazole, 200 mM NaCl, 1 mM $MgCl_2$, 10% Glycerol, 0.005% TritionX-100), ion exchange chromatography start buffer (25 mM HEPES-NaOH pH7.5, 100 mM NaCl, 1 mM $MgCl_2$, 10% Glycerol, 0.005% TritionX-100) and ion exchange chromatography elution buffer (start buffer containing 1 M NaCl).

4.3.3. Kinetic analysis of enzymatic activity

Kinetic analysis was carried out in 50 mM Tris-HCl pH7.5, 50 mM NaCl, 30 mM

$MgCl_2$, 0.1 mM EGTA, 0.02% 2-mercaptoethanol, with 2 nM His-PPM1D(1-420). Substrate sequences were Ac-VEPPLS(P)QETFSDLW-NH_2. Parameters of Michaelis-Menten equation were calculated by fitting data points with KaleidaGraph4.0 (HULINKS, Japan). Michaelis-Menten equation is followed.

$$v = (V_{max})\,[S] / (K_m + [S])$$

4.3.4. Size exclusion chromatography analysis

PPM1D were analyzed with Superdex 200 (GE healthcare, England) with SEC elution buffer (25 mM HEPES-NaOH pH6.8, 500 mM NaCl, 1 mM $MgCl_2$, 10% Glycerol, 0.005% TritionX-100)

4.4. Results

4.4.1. Effect of the PPM1D specific P-loop on micronucleoli formation

To analyze the contribution of the PPM1D specific P-loop on the nucleolus and the micronucleoli formation, the P-loop was replaced with the corresponding sequence of PPM1A, another PPM1 family isoform, and this substitution mutant was named as Sub-P1 and SubP2, respectively (**Figure 4-1**). Prediction of second structure of P-loop indicated a turn structure in P-loop. Sub-P2 has the estimated turn but not SubP-1. Stably expressing PPM1D mutants were established using the H1299 cell line, which is a human non-small lung cancer cell line. Western blotting analysis confirmed PPM1D protein level of each stable cell line (**Figure 4-2, Table 4-1**). I next analyzed the numbers of nucleoli in a nucleus, and the relation between PPM1D level and nucleoli number is shown in **Table 4-1**. Percentages of cell with micronucleoli were also analyzed. Nucleoli number and percentages of cell with micronucleoli were increased in PPM1D overexpressing cell line whereas percentages of cell cycle stages are almost the same among each cell line (**Figure 4-3**). Interestingly, the nucleolar numbers were increased in SubP1 and Sub2 stable cell lines compared with PPM1D WT. Notably, SL-176 treatment decreased the effects of P-loop substitution on the nucleolar number and micronucleolar formation, indicating that the P-loop may regulate PPMD activity (**Table 4-1**).

4.4.2. Regulation of PPM1D specific P-loop on phosphatase activity of PPM1D

Pro-rich regions are important regions for protein-protein interactions. I next analyzed PPM1D oligomerization by size exclusion chromatography. The His-tag fused

PPM1D catalytic domain was expressed in *E. coli*. Proteins purified with His-affinity and ion exchange chromatography were then analyzed by gel filtration chromatography. Purities of purified samples were confirmed with SDS-PAGE analysis (**Figure 4-4**). The elution peak of His-PPM1D(1-420) contained oligomer and monomer peaks (**Figure 4-5**). However His-PPM1D(1-420) SubP1 scarcely formed oligomers. Kinetics analysis of each peak was also performed. The K_m value of oligomers and monomers were almost the same toward substrate peptides (**Figure 4-6, Table 4-3**). The K_m value of oligomers and monomers suggested that the affinity of protein and substrate did not change, meaning that structure of the substrate binding site of His-PPM1D(1-420) is the same as His-PPM1D SubP1. On the other hand, the k_{cat} value of oligomer decreased to 26%. These data suggest that PPM1D may be regulated negatively via homo-oligomer formation.

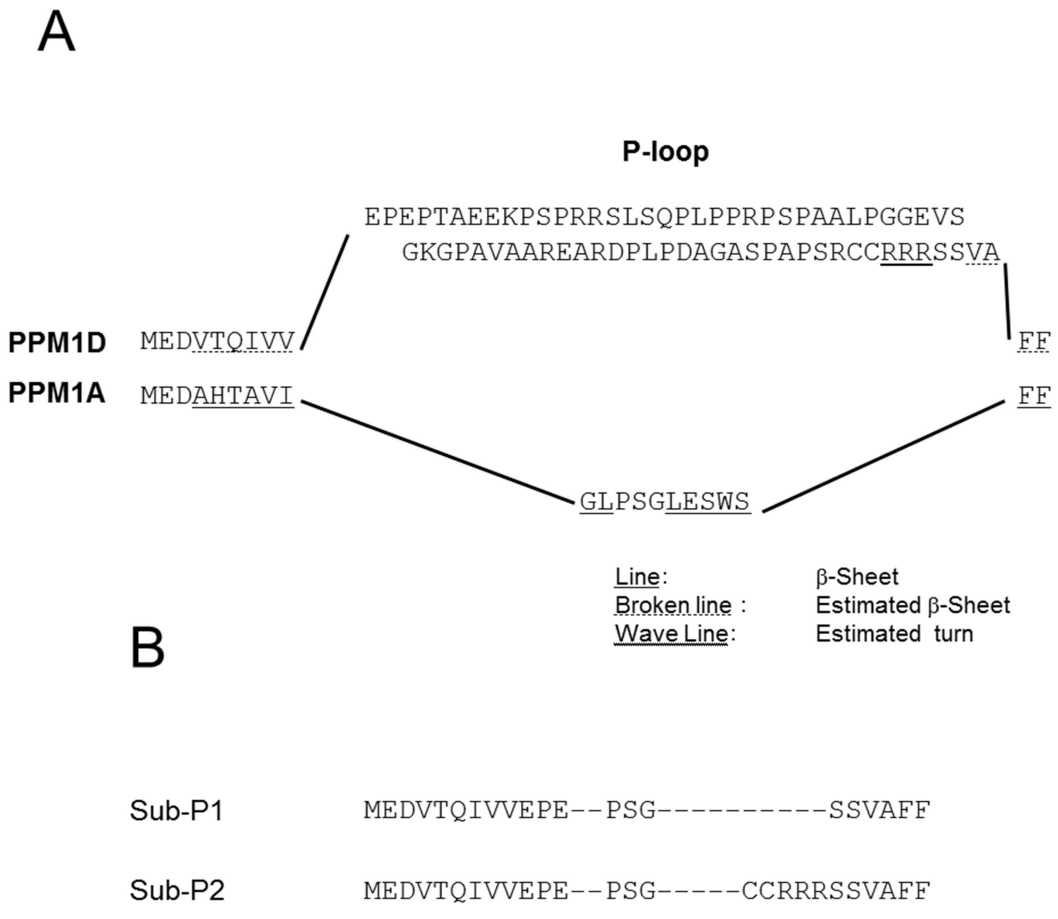

Figure 4-1 Sequence comparison of PPM1D P-loop with PPM1A

A) Sequence of PPM1D P-loop. Line is sequence whish forms β-sheet in crystal structure of PM1A. Broken and wave line are estimated β-sheet and turn region, respectively. B) Sequence of Sub-P1 and SubP2.

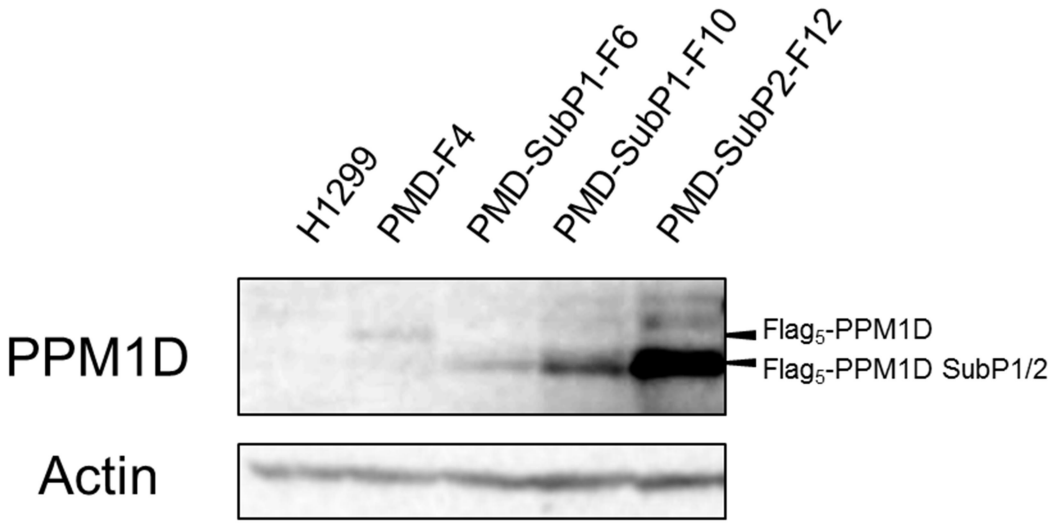

Figure 4-2 Expression level of PPM1D in stable clones

$Flag_5$ tagged PPM1D SubP1/2 were expressed in H1299 PMD-SubP1-F6, H1299 PMD-SubP1-F10 and H1299 PMD-SubP2-F12. Actin was used for loading control.

Table 4-1 Repression of micro-nucleolus in H1299 clones by SL-176

PPM1D Level (% of MCF7)	Clone	Treatment	Micro-nucleolus (%)	Number of Nucleoli	n
4	H1299	No treat	2.9	3.8 ± 0.1	722
		Vehicle	3.0	3.7 ± 0.1	823
		SL-176	2.6	3.8 ± 0.2	906
13	PMD-F4	No treat	5.9	4.1 ± 0.1	743
		Vehicle	5.7	4.2 ± 0.1	846
		SL-176	3.3	3.9 ± 0.1	810
11	PMD-SubP1-F6	No treat	8.1	5.1 ± 0.1	595
		Vehicle	7.1	5.0 ± 0.1	694
		SL-176	4.7	4.3 ± 0.2	716
14	PMD-SubP1-F10	No treat	7.1	4.8 ± 0.2	578
		Vehicle	7.6	4.7 ± 0.1	580
		SL-176	4.9	4.1 ± 0.2	617
24	PMD-SubP2-F12	No treat	7.2	5.0 ± 0.1	917
		Vehicle	7.0	4.2 ± 0.1	1001
		SL-176	3.8	4.2 ± 0.1	927

Data were analyzed by counting the cells which have the micro-nucleolus. Total cell numbers were shown on table. Concentration of Sl-176 was 2 μM.

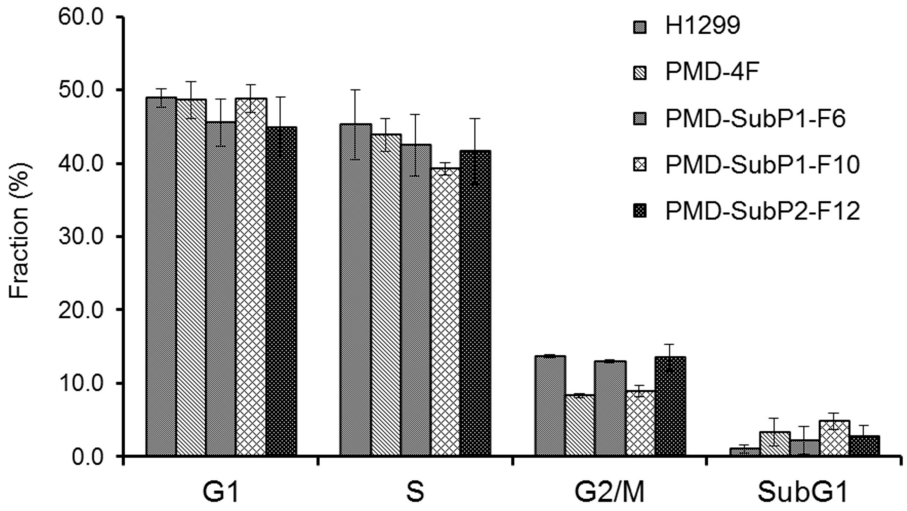

Figure 4-3 Cell cycle of H1299 and PPM1D SubP1/2 stable clones

Cell cycle of H1299 PMD-9, H1299 PMD-12, H1299 PMD-F4, PMD-SubP1-F6, H1299 PMD-SubP1-F10 and H1299 PMD-SubP2-F12 was analyzed with flow cytometory. Data represent the mean ± S.D. of 3 independent experiments.

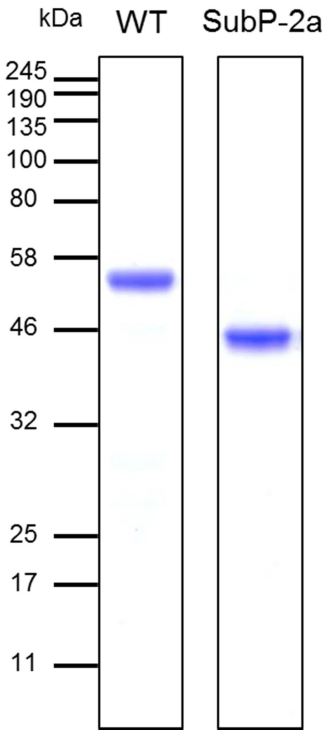

Figure 4-4 SDS-PAGE of His-PPM1D(1-420) WT and His-PPM1D(1-420) SubP1

Protein was detected with CBB staining.

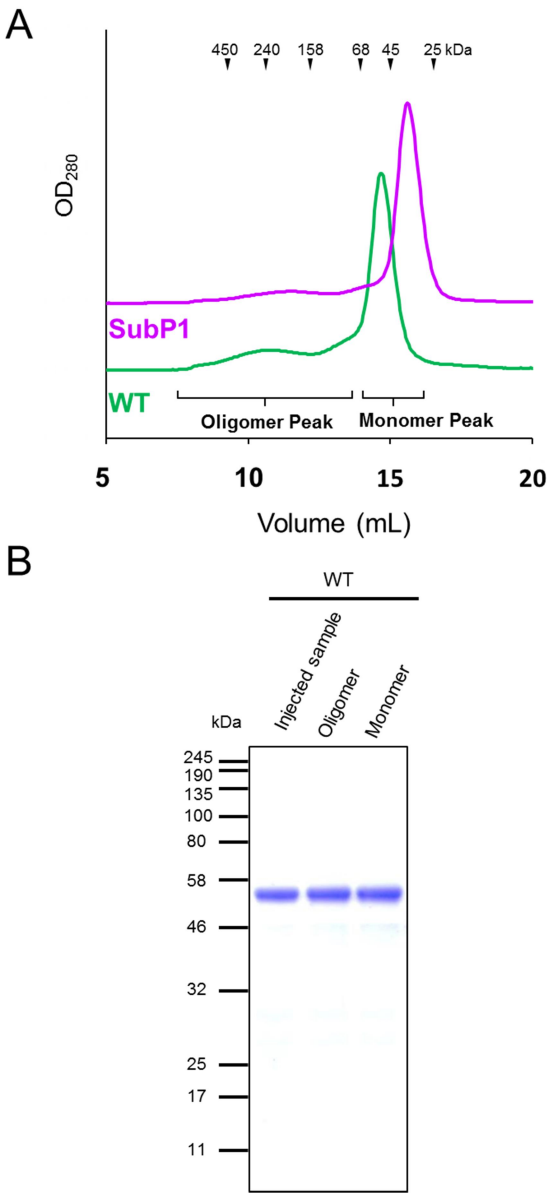

Figure 4-5 Oligomer formation of His-PPM1D(1-420)

A) Analysis of oligomerization of PPM1D by SEC. Fractions were collected as oligomer peak and monomer peak. Analysis was performed at 4°C. B) SDS-PAGE of fractions of oligomer peak and monomer peak. Protein was detected with CBB staining.

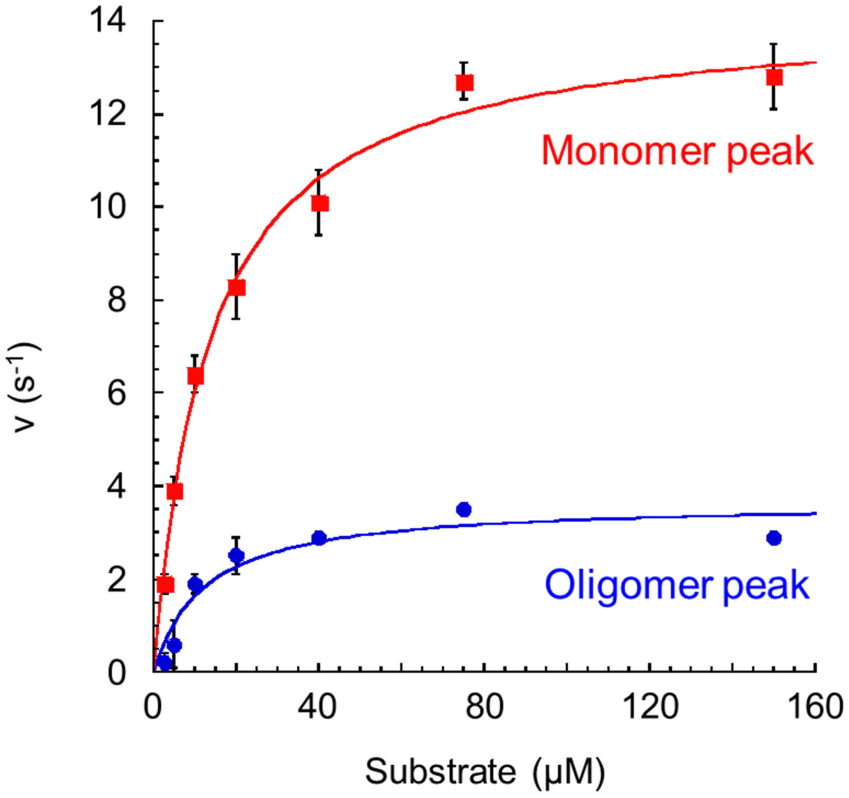

Figure 4-6 Kinetic analysis of oligomer and monomer peak of His-PPM1D(1-420)

Kinetic analysis was performed toward Ac-VEPPLS(P)QETFSDLW-NH_2 peptide which is PPM1D target sequence derived from p53. Enzyme concentrations were 2 nM. Data represent the mean ± S.D. of 3 points, respectively, from independent experiments.

Table 4-2 Parameter of kinetic analysis of PPM1D oligomer and monomer

Peak	K_m (μM)	k_{cat} (s^{-1})	k_{cat} / K_m (x 10^6 $s^{-1}M^{-1}$)
Oligomer	12.5 ± 4.8	3.7 ± 0.4	0.29
Monomer	13.6 ± 1.5	14.2 ± 0.5	1.04

Data were calculated by data of figure 3-5. Values of ± were fitting errors.

4.5. Discussion

This study demonstrated that PPM1D regulates the nucleolar number and micronucleolar formation. I also identified P-loop as a regulation region of PPM1D. *In vitro* analysis showed oligomer formation of PPM1D via the P-loop. Kinetic analysis of phosphatase activity suggested that oligomerization negatively regulates PPM1D turnover but not affinity to substrate. A previous study reported the dimerization of cyanobacterial PPM1 phosphatase (*11*). This indicates that homo-interaction of PPM1 family members is conserved among PPM1 orthologs. Ser4 and Thr199 of NPM affect micronucleolar formation. Ser4 and Thr199 are phosphorylated by CDK1 and PLK1 kinase, which are activated by PPM1D and dependent on PPM1D phosphatase activity (*12*). P-loop substitution mutants enhanced the nucleolar number and micronucleolar formation, and the enhanced effects were inhibited by the SL-176 PPM1D inhibitor. Therefore, substitution effects of P-loop were associated with upregulation of PPM1D phosphatase activity.

The P-loop contains four phosphorylation sites (*13*) (**Table 4-3**). Two sites, Ser54 and Ser96, have been characterized as destabilization factors of PPM1D (*13*). In addition, phosphorylation prediction based on kinase motifs proposed six phosphorylated sites in the P-loop (*14*). Taken together, 7 sites in the P-loop, which comprise 9.9% (7/71) of amino acid residues of the P-loop, could be phosphorylated. In a mutation database of tumors, 7 mutations in the P-loop residue have been reported (*15*) (**Table 4-4**). These reports suggested the P-loop is an important regulation region of PPM1D. Taken together, these findings suggest that PPM1D is negatively regulated by oligomerization via the P-loop. Further study is required to clarify the mechanism of PPM1D oligomerization via posttranslational modifications of the P-loop.

Table 4-3. Phosphorylation site of P-loop

Position	Sequence	Report	Proteomics	Motif Prediction	Reported Kinase	Predicted kinase
Ser40	AEEKPSPRRSL		5	1		p38 MAPK, GSK3
Ser44	PSPRRSLSQPL			1		PKA
Ser46	PRRSLSQPLPP		1	1		RSK, ATM, PKA
Ser54	LPPRPSPAALP	1		1	HIPK2	PKA, GSK3
Ser85	PDAGASPAPSR	1	3		HIPK2	
Ser96	RCRRRSSVAFF			1		PKA
Ser97	CRRRSSVAFFF			1		PKC

Ser54 and Ser85 were reported as HIKP2 kinase target. Proteomics analysis showed Ser40, Ser46 and Ser85 were phosphorylated. Prediction based kinase motif proposed that 6 sites are phosphorylated by p38 MAPK, GSK3, PKA, ATM and/or PKC kinase. In sequences, green, red and blue letter are hydrophilic, acidic and basic amino residue, respectively.

Table 4-4. **Missense mutations of P-loop in tumors**

Position	Mutation	Tumor
64	S64L	Pancreas cancer
70	V70M	Lung adenocarcinoma
86	P86Q	Thyroid cancer
88	P88S	Hematopoietic neoplasm
92	C92R	Colorectal cancer
93	R93L	Brest carcinoma
95	R95S	Liver cancer

Reference: Gao *et al.* (*15*)

4.6. References

1. D. V. Bulavin, O. N. Demidov, S. Saito, P. Kauraniemi, C. Phillips, S. A. Amundson, C. Ambrosino, G. Sauter, A. R. Nebreda, C. W. Anderson, A. Kallioniemi, A. J. Fornace, Jr., E. Appella (2002) Amplification of PPM1D in human tumors abrogates p53 tumor-suppressor activity Nat Genet, 31, 210-215.
2. G. B. Li, X. L. Zhang, L. Yuan, Q. Q. Jiao, D. J. Liu, J. Liu (2013) Protein phosphatase magnesium-dependent 1delta (PPM1D) mRNA expression is a prognosis marker for hepatocellular carcinoma PLoS One, 8, e60775.
3. P. Loukopoulos, T. Shibata, H. Katoh, A. Kokubu, M. Sakamoto, K. Yamazaki, T. Kosuge, Y. Kanai, F. Hosoda, I. Imoto, M. Ohki, J. Inazawa, S. Hirohashi (2007) Genome-wide array-based comparative genomic hybridization analysis of pancreatic adenocarcinoma: identification of genetic indicators that predict patient outcome Cancer Sci, 98, 392-400.
4. D. S. Tan, M. B. Lambros, S. Rayter, R. Natrajan, R. Vatcheva, Q. Gao, C. Marchio, F. C. Geyer, K. Savage, S. Parry, K. Fenwick, N. Tamber, A. Mackay, T. Dexter, C. Jameson, W. G. McCluggage, A. Williams, A. Graham, D. Faratian, M. El-Bahrawy, A. J. Paige, H. Gabra, M. E. Gore, M. Zvelebil, C. J. Lord, S. B. Kaye, A. Ashworth, J. S. Reis-Filho (2009) PPM1D is a potential therapeutic target in ovarian clear cell carcinomas Clin Cancer Res, 15, 2269-2280.
5. F. Saito-Ohara, I. Imoto, J. Inoue, H. Hosoi, A. Nakagawara, T. Sugimoto, J. Inazawa (2003) PPM1D is a potential target for 17q gain in neuroblastoma Cancer Res, 63, 1876-1883.
6. D. V. Bulavin, C. Phillips, B. Nannenga, O. Timofeev, L. A. Donehower, C. W. Anderson, E. Appella, A. J. Fornace, Jr. (2004) Inactivation of the Wip1 phosphatase inhibits mammary tumorigenesis through p38 MAPK-mediated activation of the p16(Ink4a)-p19(Arf) pathway Nat Genet, 36, 343-350.
7. Y. Shi (2009) Serine/threonine phosphatases: mechanism through structure Cell, 139, 468-484.
8. Y. Chuman, H. Yagi, T. Fukuda, T. Nomura, M. Matsukizono, Y. Shimohigashi, K. Sakaguchi (2008) Characterization of the active site and a unique uncompetitive inhibitor of the PPM1-type protein phosphatase PPM1D Protein Pept Lett, 15, 938-948.
9. M. P. Williamson (1994) The structure and function of proline-rich regions in proteins Biochem J, 297 (Pt 2), 249-260.
10. B. K. Kay, M. P. Williamson, M. Sudol (2000) The importance of being proline: the interaction of proline-rich motifs in signaling proteins with their cognate domains FASEB J, 14, 231-241.
11. Y. L. Si, Y. Yuan, Y. Wang, J. Gao, Y. B. Hu, S. Q. Feng, J. Y. Su (2016) Structural and Biochemical Characterization of a Cyanobacterial PP2C Phosphatase Reveals Insights into Catalytic Mechanism and Substrate Recognition Catalysts, 6.
12. Y. Kozakai, R. Kamada, J. Furuta, Y. Kiyota, Y. Chuman, K. Sakaguchi (2016) PPM1D controls nucleolar formation by up-regulating phosphorylation of nucleophosmin Sci Rep, 6, 33272.

13. D. W. Choi, W. Na, M. H. Kabir, E. Yi, S. Kwon, J. Yeom, J. W. Ahn, H. H. Choi, Y. Lee, K. W. Seo, M. K. Shin, S. H. Park, H. Y. Yoo, K. Isono, H. Koseki, S. T. Kim, C. Lee, Y. K. Kwon, C. Y. Choi (2013) WIP1, a homeostatic regulator of the DNA damage response, is targeted by HIPK2 for phosphorylation and degradation Mol Cell, 51, 374-385.
14. N. Blom, T. Sicheritz-Ponten, R. Gupta, S. Gammeltoft, S. Brunak (2004) Prediction of post-translational glycosylation and phosphorylation of proteins from the amino acid sequence Proteomics, 4, 1633-1649.
15. J. Gao, B. A. Aksoy, U. Dogrusoz, G. Dresdner, B. Gross, S. O. Sumer, Y. Sun, A. Jacobsen, R. Sinha, E. Larsson, E. Cerami, C. Sander, N. Schultz (2013) Integrative analysis of complex cancer genomics and clinical profiles using the cBioPortal Sci Signal, 6, pl1.

5. Conclusions

5.1. Conclusions

Morphologies of the nucleolus are important cytodiagnostic criteria for tumor malignancy. Increase of the nucleolar number is observed in malignant tumors. In various tumors, protein overexpression and gene amplification of the proto-oncogene PPM1D have been reported. As with nucleolar number, overexpression of PPM1D is also a poor clinical prognosis marker of gastric, lung and colorectal cancer (*1-3*). PPM1D was identified as a regulation factor of the nucleolar number in our previous study (*4*). Overexpression of PPM1D increases the nucleolar number via phosphorylation of NPM. The CDC25C-CDK1-PLK1 pathway activated by PPM1D phosphorylates NPM at Ser4 and Thr199. Our study suggested a relationship between nucleolar regulation and function and PPM1D and indicated that PPM1D is an attractive target for anti-cancer chemotherapy.

The findings from this study propose a regulation mechanism of NPM oligomerization state by PPM1D. Phosphorylation of Ser4 and Thr199 NPM, which are regulated by PPM1D, destabilize decamer formation of NPM. Destabilization of NPM decamers induced an increase of the nucleolar number and formation of micronucleoli, named by our group as NPM foci in the nucleus. PNB is a structure in nucleus that is formed in early G1 phase (*5*). PNB is observed as NPM foci, and resembles micronucleoli. Phosphorylation of Thr199 in NPM decreases ribosome biosynthesis (*6*), and the main functions of the nucleolus and PNB are ribosomal biosynthesis (*7*). Taken together, I propose a hypothesis by which phosphorylated NPM on Ser4 and Thr199 prevents formation of the nucleolus and PNBs.

The P-loop was identified as a regulation region of the nucleolar number. Oligomer formation of PPM1D via P-loop could regulate its phosphatase activity, negatively. Regulation mechanisms of PPM1D are not clarified. This study proposed a novel regulation mechanism of PPM1D phosphatase activity. Additionally, Ser54 and Ser96 on P-loop were reported as posttranslational modification sites (*8*) The P-loop contains phosphorylation sites as reported by proteomics analysis (*9-14*), and PPM1D oligomer formation may be regulated by these phosphorylation sites. SL-176 repressed the increase of nucleoli number regardless of P-loop substitution. This indicates that SL-176 can inhibit PPM1D even if PPM1D is activated by oligomer destabilization. SL-176 effectively decreased the nucleolar number. This study suggested that SL-176 is a hopeful lead compound for chemotherapy targeting the increase of the nucleolar number.

Taken together, I propose a regulation model of the nucleolar formation via PPM1D (**Figure 6-1**). Overexpressed PPM1D increases NPM phosphorylation on Ser4 and Thr199 via activation of CDK1 and PLK1. Phosphorylated NPM is destabilized for decamer formation, suggesting that interaction of NPM to binding factors should be weakened. As a result, PPM1D induces the micronucleolus and nucleolar number. P-loop also negatively regulates PPM1D activity, and the P-loop contains phosphorylated sites. Modifications at the P-loop could affect the nucleolar number via PPM1D regulation. These results suggest that the P-loop of PPM1D can be a target for anti-cancer therapy. Both the nucleolar number and PPM1D overexpression are prognosis markers of malignant tumors. The model proposes a relationship between PPM1D and nucleolar number without the tumor suppressor protein p53. SL-176 inhibits PPM1D activity and represses the nucleolar number, suggesting that SL-176

can be used as a lead compound of chemotherapy for p53-negative tumors.

In summary, this study proposes a model by which PPM1D regulates the nucleolus via NPM oligomerization. The P-loop is a regulation region of PPM1D and affects nucleolus formation. SL-176 is a PPM1D specific inhibitor that represses proliferation of PPM1D overexpressing cells. SL-176 also decreases the nucleolar number. SL-176 is useful as a lead compound for anti-cancer chemotherapy. To develop a novel cancer chemotherapy strategy, a relationship between the increase of the nucleolar number, which is regulated by PPM1D, and tumor prognosis should be examined.

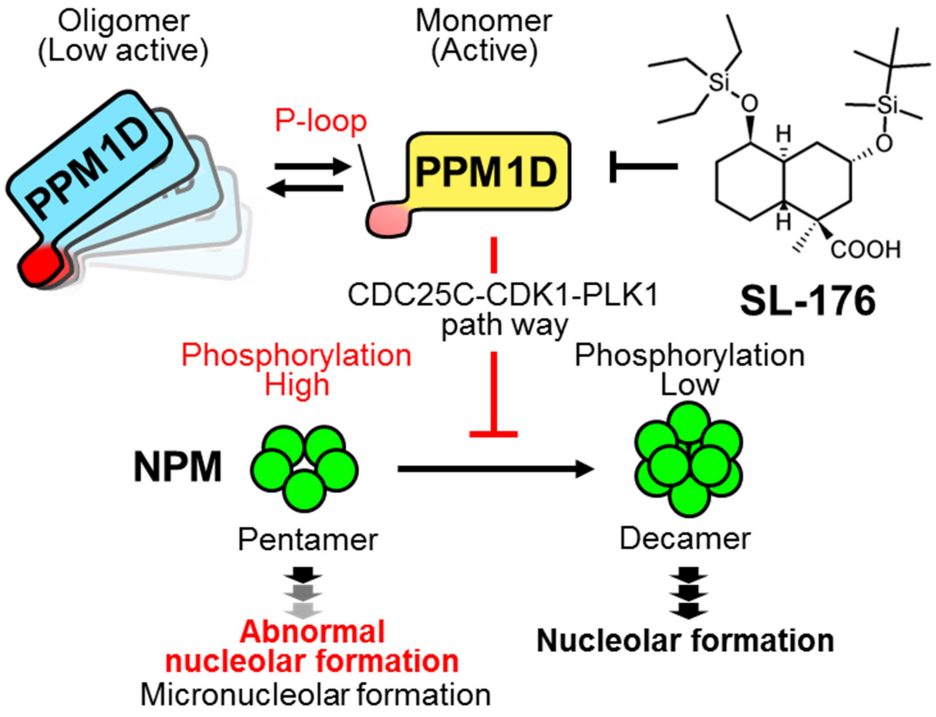

Figure 5-1 Model of increase of the nucleolus by PPM1D

PPM1D inhibits maturation of the nucleolus via destabilization of NPM decamer. Destabilization of NPM by PPM1D. PPM1D is negativity regulated by its P-loop though oligomerization.

5.2. References

1. G. B. Li, X. L. Zhang, L. Yuan, Q. Q. Jiao, D. J. Liu, J. Liu (2013) Protein phosphatase magnesium-dependent 1delta (PPM1D) mRNA expression is a prognosis marker for hepatocellular carcinoma PLoS One, 8, e60775.
2. F. Saito-Ohara, I. Imoto, J. Inoue, H. Hosoi, A. Nakagawara, T. Sugimoto, J. Inazawa (2003) PPM1D is a potential target for 17q gain in neuroblastoma Cancer Res, 63, 1876-1883.
3. D. S. Tan, M. B. Lambros, S. Rayter, R. Natrajan, R. Vatcheva, Q. Gao, C. Marchio, F. C. Geyer, K. Savage, S. Parry, K. Fenwick, N. Tamber, A. Mackay, T. Dexter, C. Jameson, W. G. McCluggage, A. Williams, A. Graham, D. Faratian, M. El-Bahrawy, A. J. Paige, H. Gabra, M. E. Gore, M. Zvelebil, C. J. Lord, S. B. Kaye, A. Ashworth, J. S. Reis-Filho (2009) PPM1D is a potential therapeutic target in ovarian clear cell carcinomas Clin Cancer Res, 15, 2269-2280.
4. Y. Kozakai, R. Kamada, J. Furuta, Y. Kiyota, Y. Chuman, K. Sakaguchi (2016) PPM1D controls nucleolar formation by up-regulating phosphorylation of nucleophosmin Sci Rep, 6, 33272.
5. C. Carron, S. Balor, F. Delavoie, C. Plisson-Chastang, M. Faubladier, P. E. Gleizes, M. F. O'Donohue (2012) Post-mitotic dynamics of pre-nucleolar bodies is driven by pre-rRNA processing J Cell Sci, 125, 4532-4542.
6. M. Hisaoka, S. Ueshima, K. Murano, K. Nagata, M. Okuwaki (2010) Regulation of nucleolar chromatin by B23/nucleophosmin jointly depends upon its RNA binding activity and transcription factor UBF Mol Cell Biol, 30, 4952-4964.
7. D. Hernandez-Verdun (2011) Assembly and disassembly of the nucleolus during the cell cycle Nucleus, 2, 189-194.
8. D. W. Choi, W. Na, M. H. Kabir, E. Yi, S. Kwon, J. Yeom, J. W. Ahn, H. H. Choi, Y. Lee, K. W. Seo, M. K. Shin, S. H. Park, H. Y. Yoo, K. Isono, H. Koseki, S. T. Kim, C. Lee, Y. K. Kwon, C. Y. Choi (2013) WIP1, a homeostatic regulator of the DNA damage response, is targeted by HIPK2 for phosphorylation and degradation Mol Cell, 51, 374-385.
9. K. Sharma, R. C. D'Souza, S. Tyanova, C. Schaab, J. R. Wisniewski, J. Cox, M. Mann (2014) Ultradeep human phosphoproteome reveals a distinct regulatory nature of Tyr and Ser/Thr-based signaling Cell Rep, 8, 1583-1594.
10. P. Mertins, J. W. Qiao, J. Patel, N. D. Udeshi, K. R. Clauser, D. R. Mani, M. W. Burgess, M. A. Gillette, J. D. Jaffe, S. A. Carr (2013) Integrated proteomic analysis of post-translational modifications by serial enrichment Nat Methods, 10, 634-637.
11. V. Mayya, D. H. Lundgren, S. I. Hwang, K. Rezaul, L. Wu, J. K. Eng, V. Rodionov, D. K. Han (2009) Quantitative phosphoproteomic analysis of T cell receptor signaling reveals system-wide modulation of protein-protein interactions Sci Signal, 2, ra46.
12. S. A. Stuart, S. Houel, T. Lee, N. Wang, W. M. Old, N. G. Ahn (2015) A Phosphoproteomic Comparison of B-RAFV600E and MKK1/2 Inhibitors in Melanoma Cells Mol Cell Proteomics,

14, 1599-1615.

13. H. Zhou, S. Di Palma, C. Preisinger, M. Peng, A. N. Polat, A. J. Heck, S. Mohammed (2013) Toward a comprehensive characterization of a human cancer cell phosphoproteome J Proteome Res, 12, 260-271.
14. M. Klammer, M. Kaminski, A. Zedler, F. Oppermann, S. Blencke, S. Marx, S. Muller, A. Tebbe, K. Godl, C. Schaab (2012) Phosphosignature predicts dasatinib response in non-small cell lung cancer Mol Cell Proteomics, 11, 651-668.

6. Acknowledgements

I would like to express my greatest appreciation to Professor Kazuyasu Sakaguchi. Without his appropriate guidance and persistent help, this thesis would not have been possible.

I would like to offer my special thanks to Professor Yota Murakami (Laboratory of Bioorganic Chemistry), Professor Seiichi Taguchi (Laboratory of Biomolecular Engineering), Professor Keiji Tanino (Laboratory of Organic Chemistry II) and assistant professor Toshiaki Imagawa (Laboratory of Biological chemistry) for their incisive comments and constructive suggestions on my paper.

I deeply appreciate collaboration of this work by Professor Keiji Tanino and Assistant Professor Fumihiko Yoshimura (Laboratory of Organic Chemistry II) who discussions on studies of the PPM1D inhibitor.

I would like to express my gratitude to Assistant Professor Rui Kamada who provided helpful comments and suggestions. I also am grateful to Associate Professor Yoshiro Chuman (Niigata University) for his honest guidance for me. I am also very grateful to all the members of the Laboratory of Biological Chemistry. I would also like to thank the Japan Chemical Industry Association for making my PhD study possible through financial support.

Finally, I would like to offer my special thanks to my family for their constant encouragement and long-term support.